ULTRAFAST OPTICS

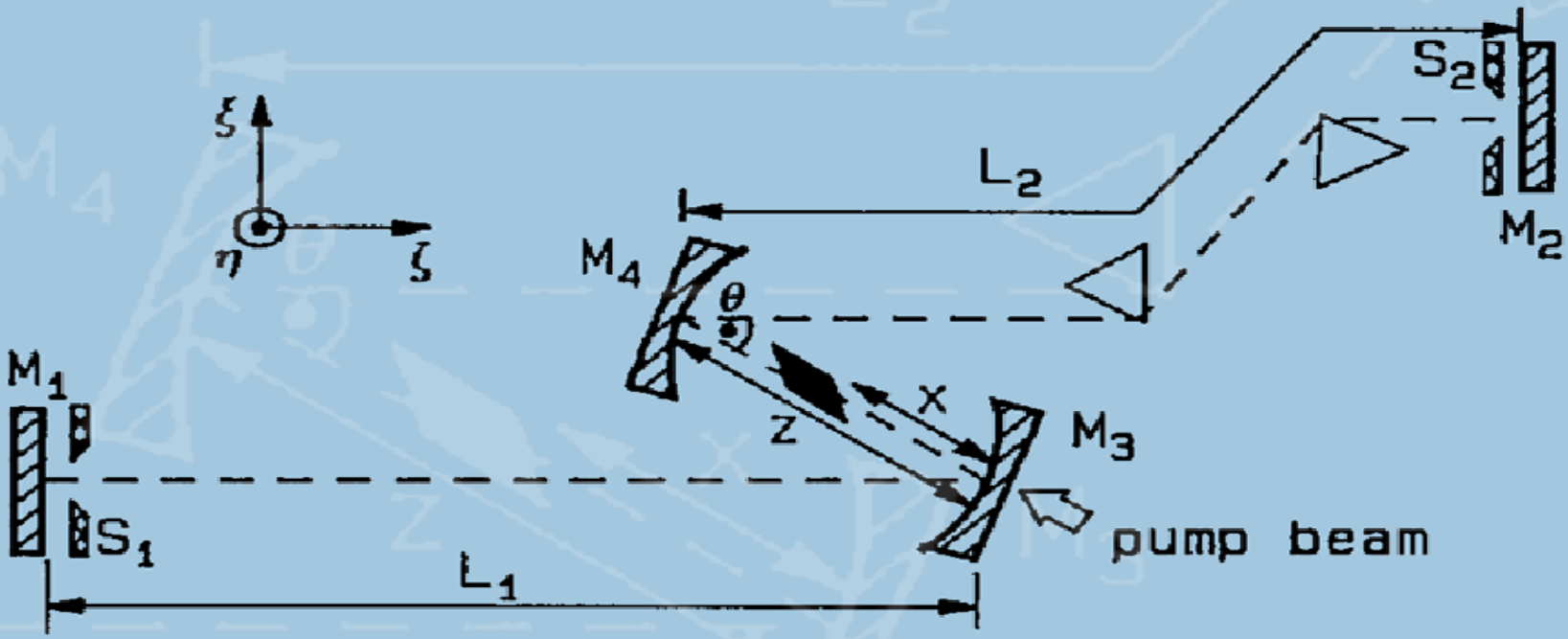

image from G. Cerullo et al., Opt. Lett. 19, 807 (1994), © OSA

by PIOTR WASYLCZYK

Second-order nonlinear optical effects – second harmonic generation

Symmetry issues

Phase-matching in SHG

Phase-matching bandwidth

Group-velocity mismatch

Nonlinear-optical crystals

Practical numbers for SHG

Electro-optics

Difference-frequency generation and optical parametric generation

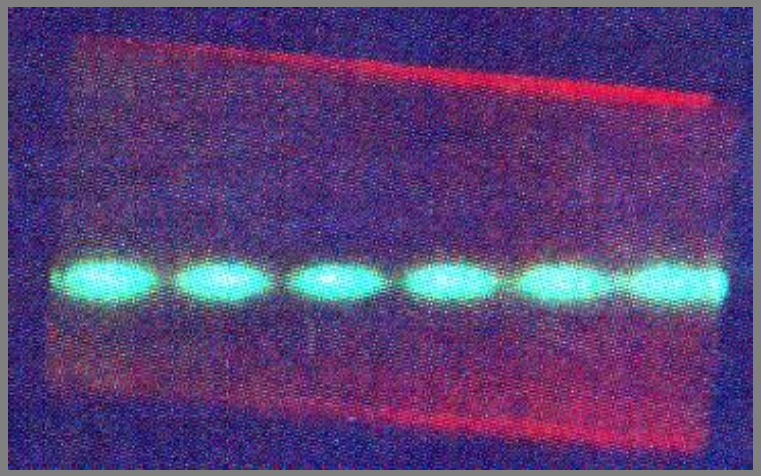

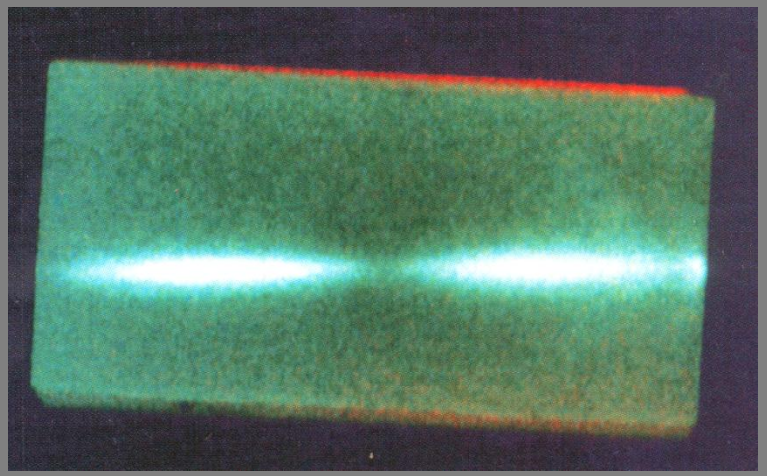

For efficient second harmonic generation you need:

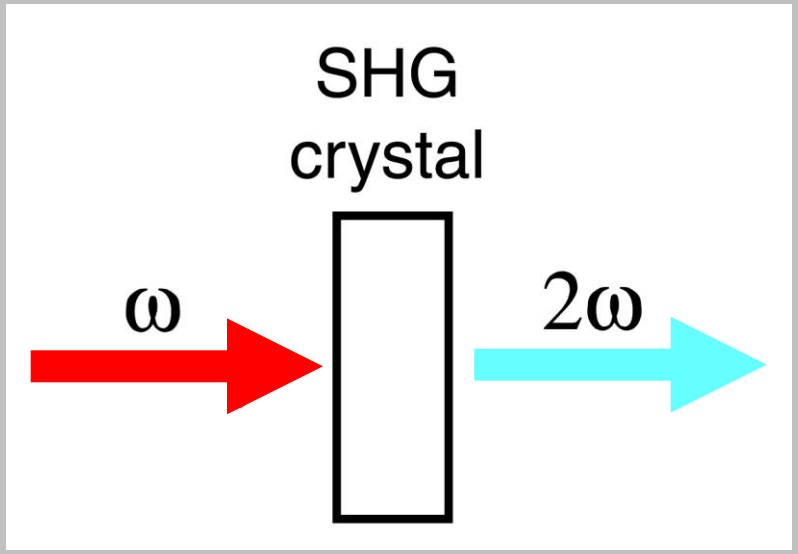

1. High **intensity** of the electric field
2. High **nonlinear response** of the medium (d_{eff})
3. Proper medium **symmetry**
4. Proper phases between contributions from different places in the medium (**phase matching**)

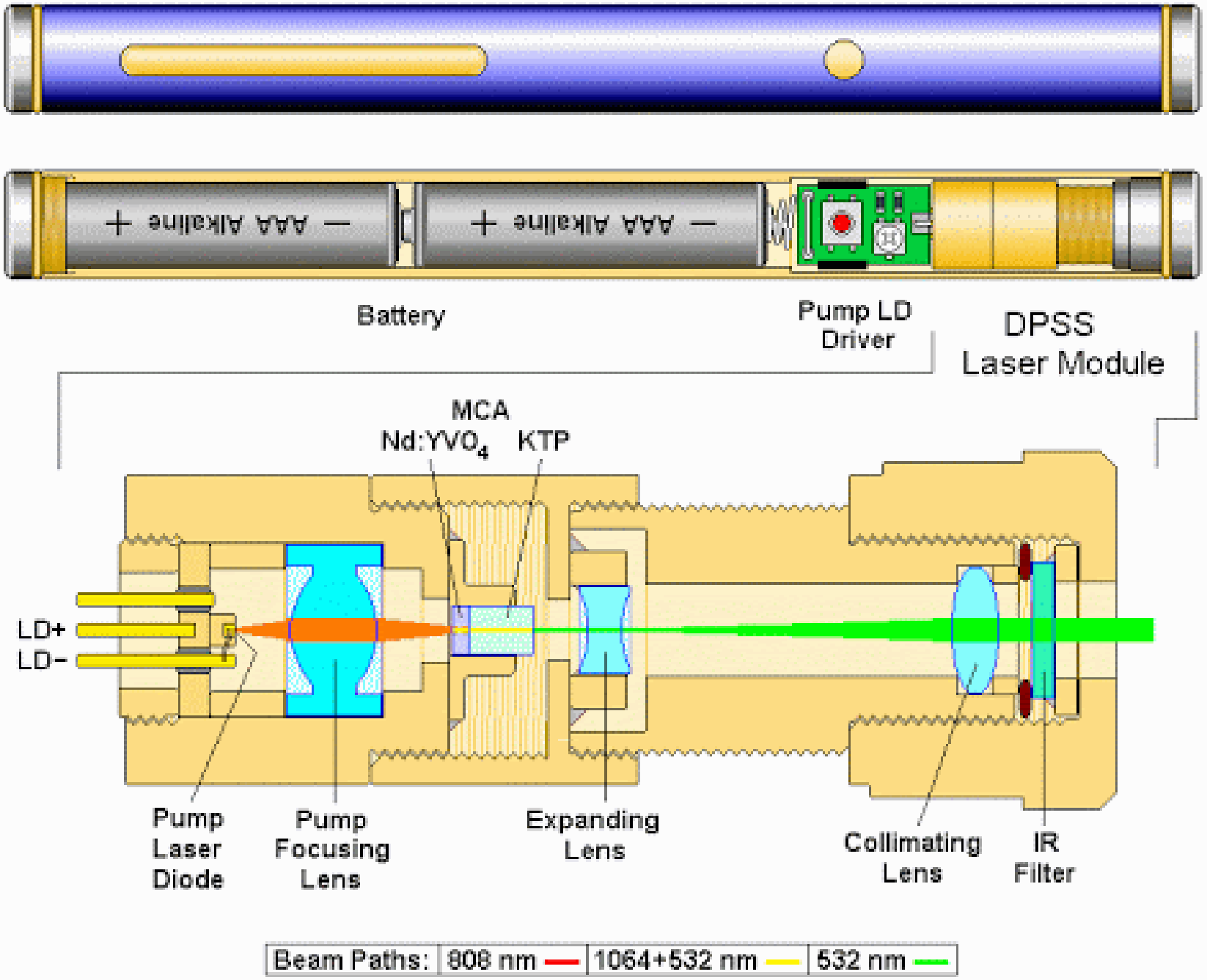
+ AAA Alkaline −
+ AAA Alkaline −
Battery
Pump LD Driver
DPSS Laser Module
MCA
Nd:YVO4
KTP
LD+
LD−
Pump Laser Diode
Pump Focusing Lens
Expanding Lens
Collimating Lens
IR Filter
Beam Paths:
808 nm
1064+532 nm
532 nm

Nonlinear electronic response

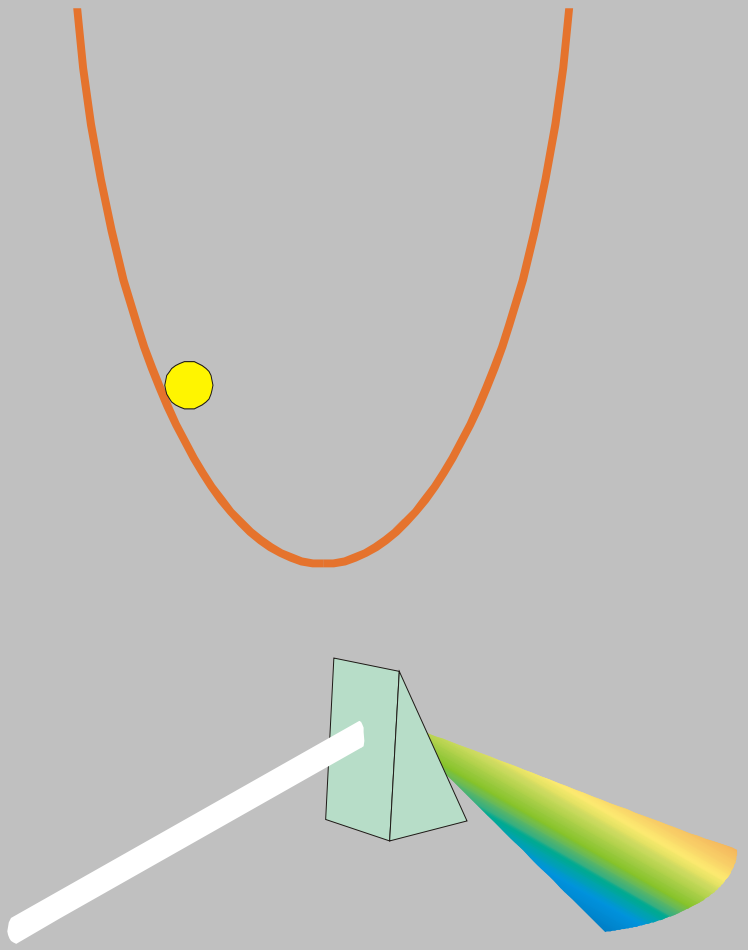

H. A. Lorentz (1909)

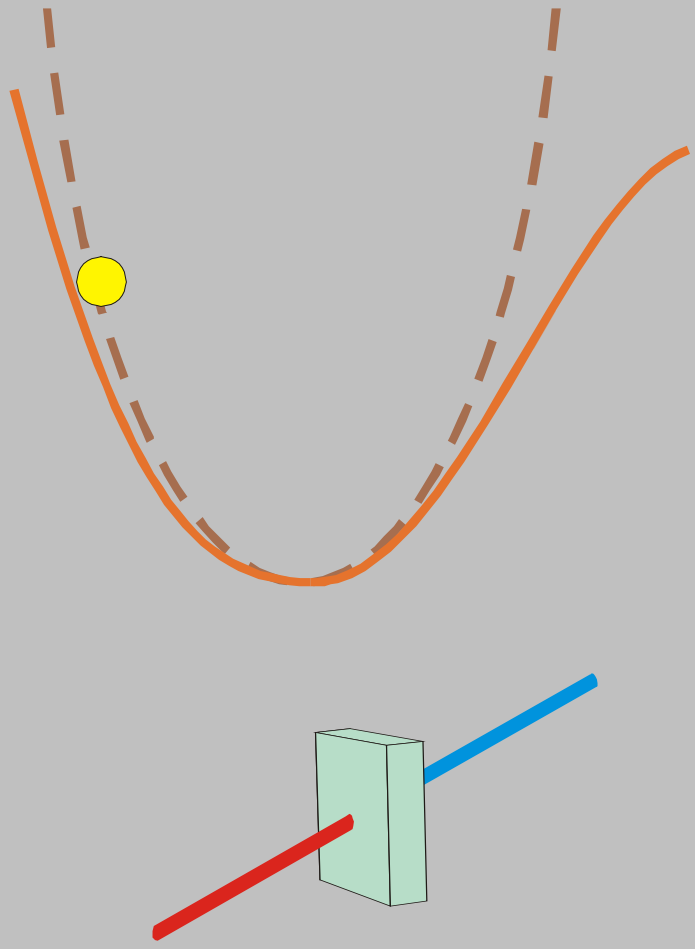

P. A. Franken (1961)

Symmetry in second-harmonic generation

$$\mathbf{E}_{sig}(x,t) \propto \chi^{(2)}\mathbf{E}^{\,2}(x,t)$$

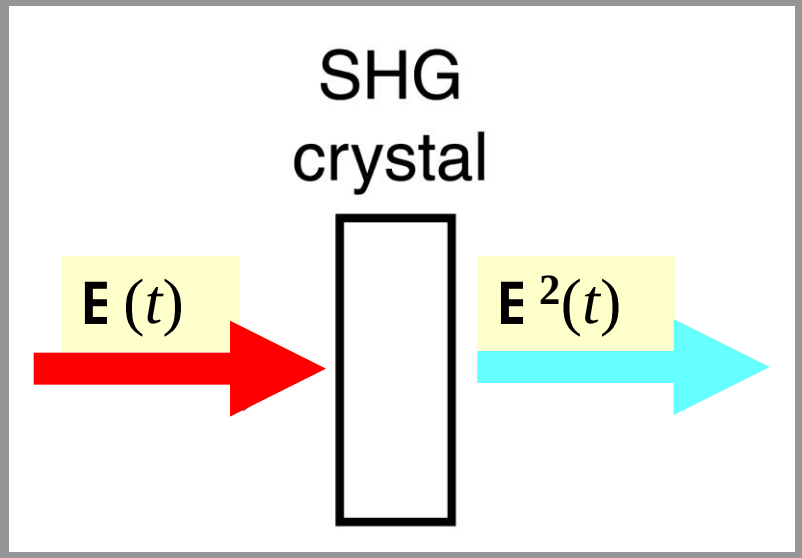

If we imagine inverting space:

$$\mathbf{E}\,(x,t) \rightarrow -\mathbf{E}\,(x,t)$$

$$\mathbf{E}_{sig}(x,t) \rightarrow -\mathbf{E}_{sig}(x,t)$$

Now, if the medium is isotropic, $\chi^{(2)}$ remains unchanged. So:

$$-\mathbf{E}_{sig}(x,t) \;\propto\; \chi^{(2)}\,[-\mathbf{E}\,(x,t)\,]^2 \;=\; \chi^{(2)}\mathbf{E}\,(x,t)^2 \;=\; \mathbf{E}_{sig}(x,t)$$

For this to hold, $\chi^{(2)}$ must be zero for media with inversion symmetry. Most materials have inversion symmetry, so you just don't see SHG—or any other even-order nonlinear-optical effect—every day.

Phase-matching in second-harmonic generation

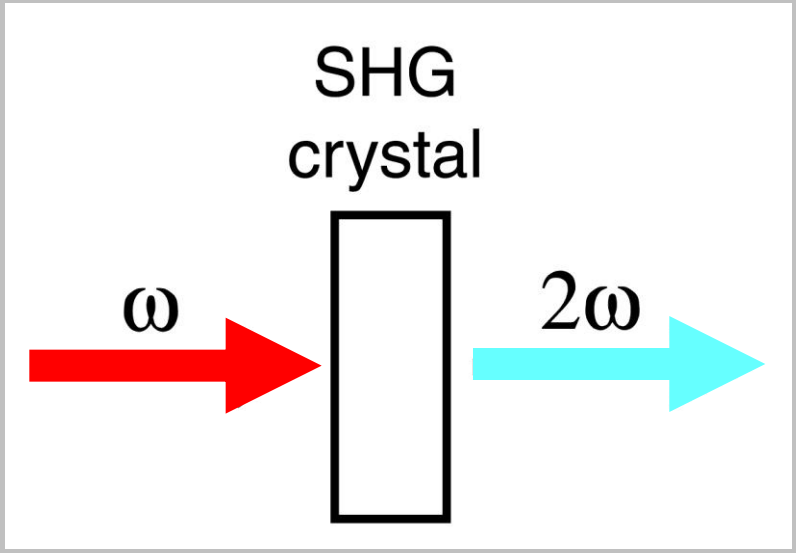

How does phase-matching affect SHG? It's a major effect, another important reason you just don't see SHG—or any other nonlinear-optical effects—every day.

First demonstration of second-harmonic generation

P.A. Franken, et al, Physical Review Letters 7, p. 118 (1961)

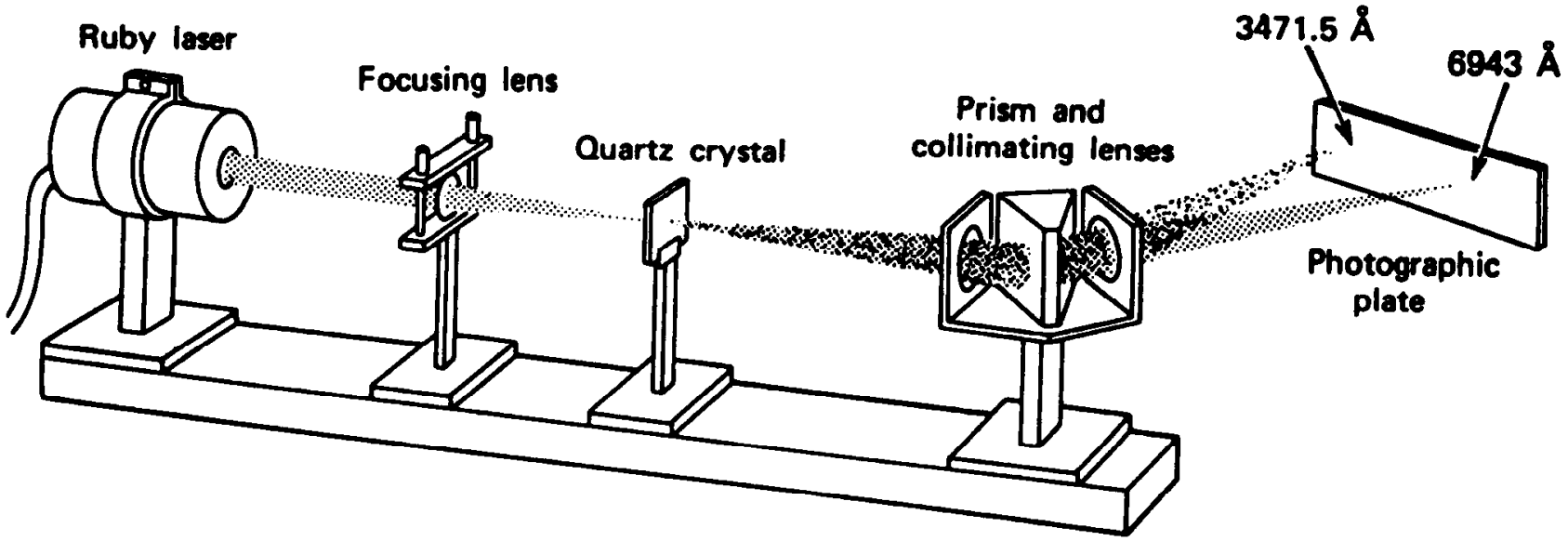

Figure 12.1. Arrangement used in the first experimental demonstration of second-harmonic generation [1]. A ruby-laser beam at $\lambda = 0.694\ \mu$m is focused on a quartz crystal, causing the generation of a (weak) beam at $\frac{1}{2}\lambda = 0.347\ \mu$m. The two beams are then separated by a prism and detected on a photographic plate.

The second-harmonic beam was very weak because the process was not phase-matched.

First demonstration of SHG: the data

The actual published results…

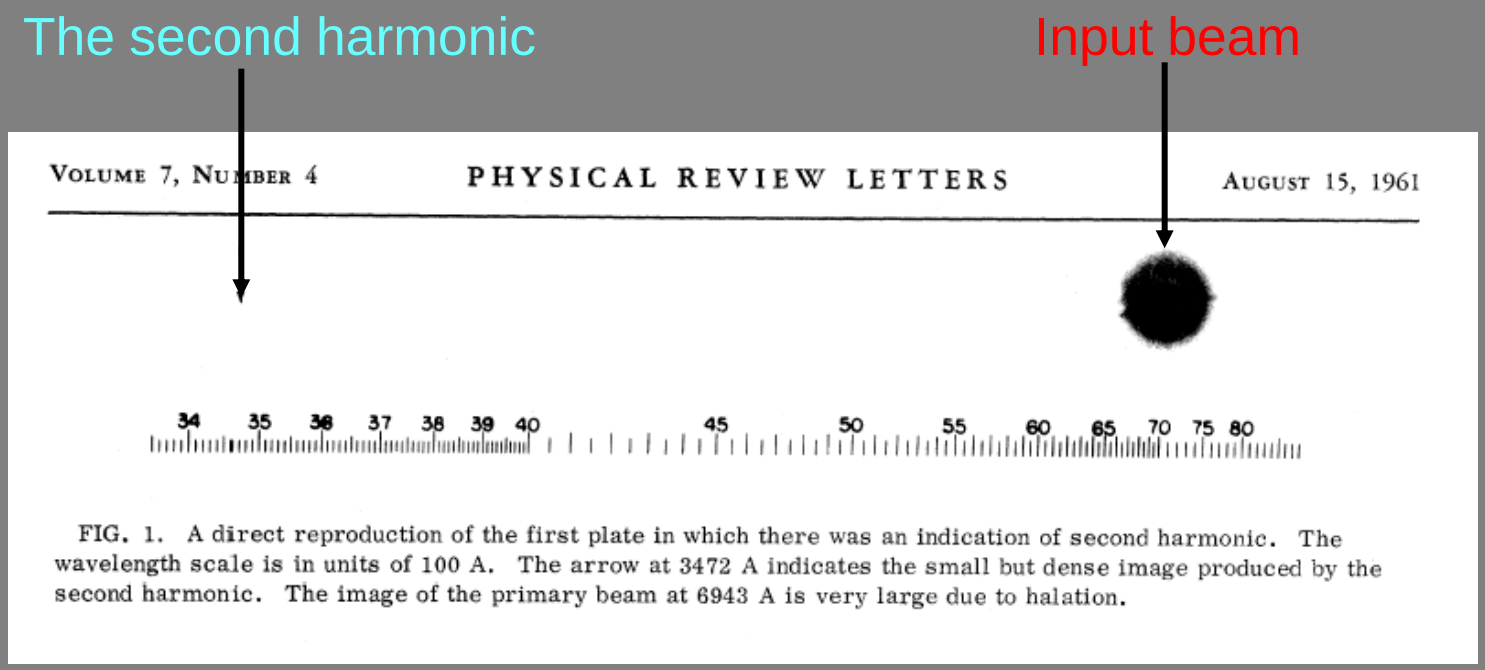

Note that the very weak spot due to the second harmonic is missing. It was removed by an overzealous Physical Review Letters editor, who thought it was a speck of dirt.

Sinusoidal dependence of SHG intensity on length

Large Δk

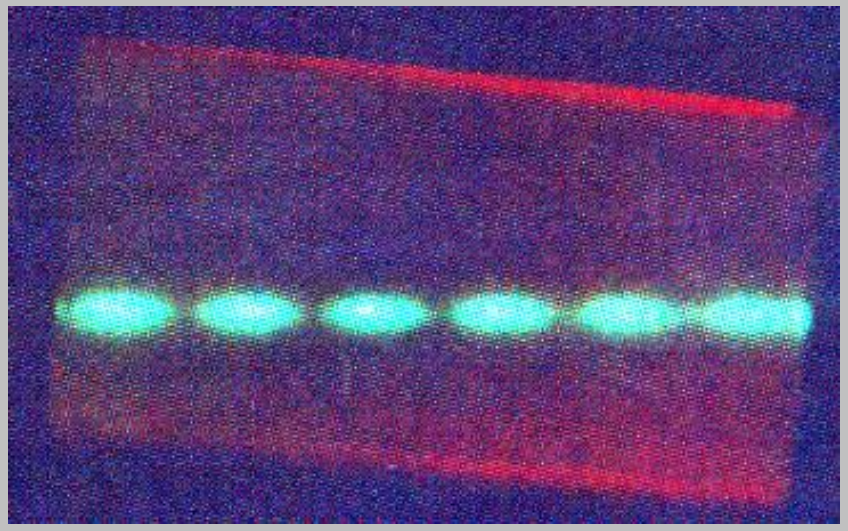

Small Δk

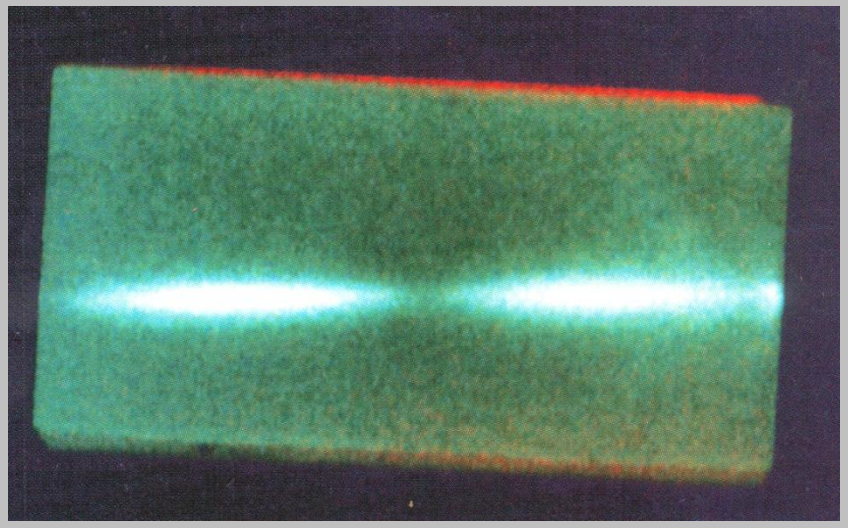

The SHG intensity is sharply maximized if $\Delta k = 0$.

Phase-matching second-harmonic generation

So we're creating light at $\omega_{sig} = 2\omega$.

The k-vector of the second-harmonic is: $k_{sig} = \frac{\omega_{sig}}{c_0} n(\omega_{sig}) = \frac{(2\omega)}{c_0} n(2\omega)$

And the k-vector of the polarization is: $k_{pol} = 2k = 2\frac{\omega}{c_0} n(\omega)$

The phase-matching condition is: $k_{sig} = k_{pol}$

which will only be satisfied when:

$$n(2\omega) = n(\omega)$$

Unfortunately, dispersion in „normal" materials, upon „normal" conditions, prevents this from ever happening!

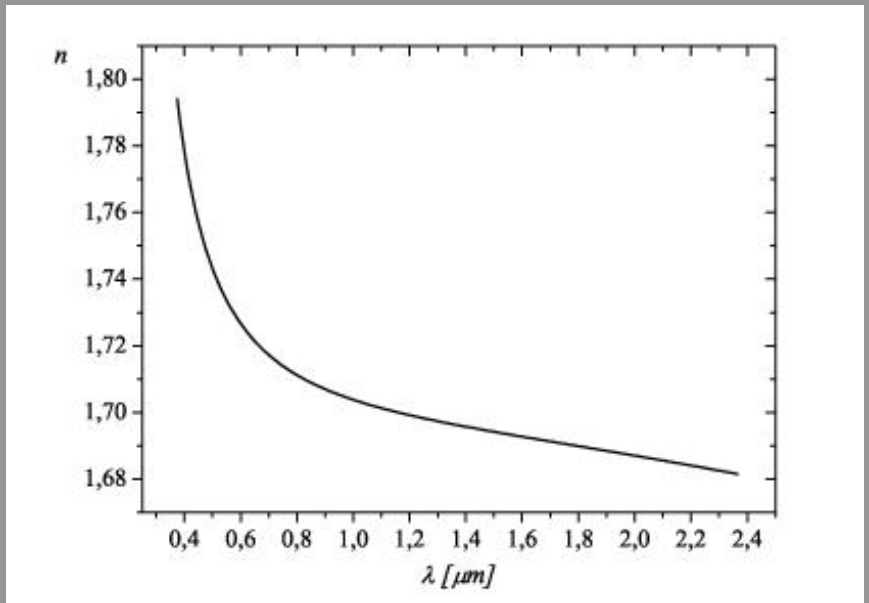

Phase-matching second-harmonic generation using birefringence

Birefringent materials have different refractive indices for different polarizations. Ordinary and extraordinary refractive indices can be different by up to ~0.1 for SHG crystals.

We can now satisfy the phase-matching condition.

Use the extraordinary polarization for ω and the ordinary for 2ω.

$$n_o(2\omega) = n_e(\omega)$$

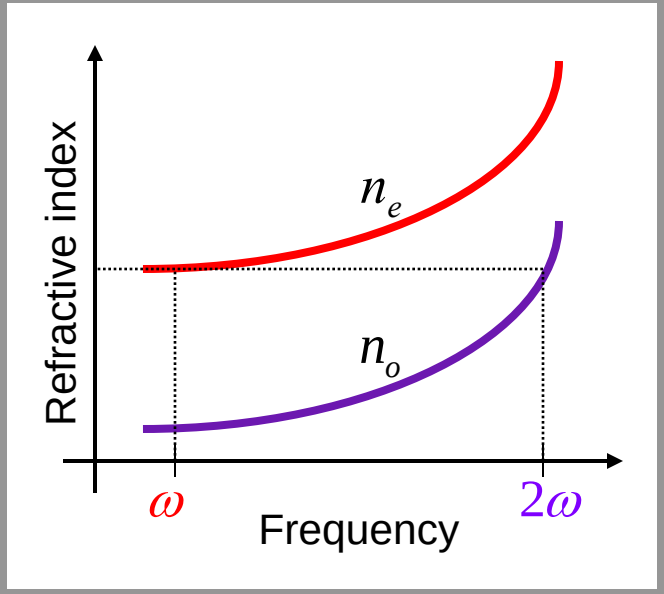

n_e depends on propagation angle, so we can tune for a given ω. Some crystals have $n_e < n_o$, so the opposite polarizations work.

Noncollinear SHG phase-matching

$$\vec{k} = k\cos\theta\,\hat{z} - k\sin\theta\,\hat{x} \longrightarrow$$

$$\vec{k}' = k\cos\theta\,\hat{z} + k\sin\theta\,\hat{x} \longrightarrow$$

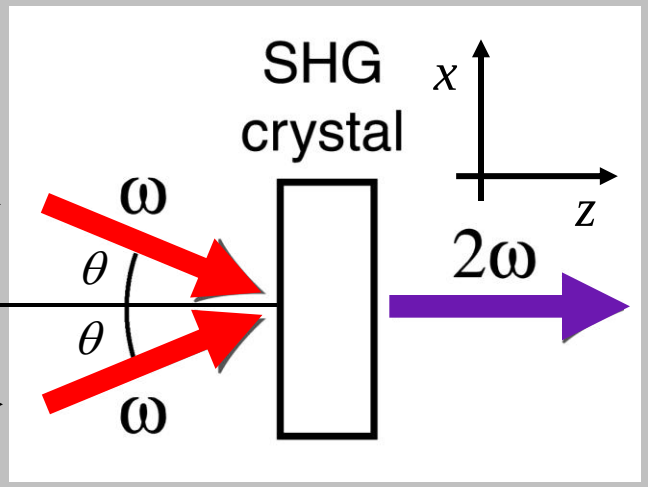

$$\vec{k}_{pol} = \vec{k} + \vec{k}' = 2k\cos\theta\,\hat{z}$$

$$\Rightarrow k_{pol} = 2\frac{\omega}{c_0}n(\omega)\cos\theta$$

But:

$$k_{sig} = \frac{2\omega}{c_o}n(2\omega)$$

So the phase-matching condition becomes:

$$n(2\omega) = n(\omega)\cos\theta$$

Phase-matching bandwidth

Recall that the intensity out of an SHG crystal of length L is:

$$I_{sig}(L) \propto (L/\lambda)^2 \,\mathrm{sinc}^2(\Delta k\, L/2)$$

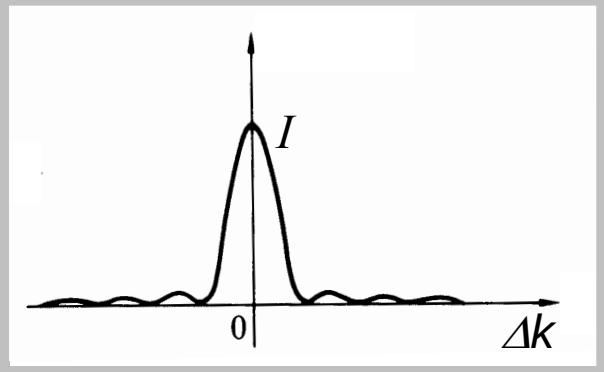

where:

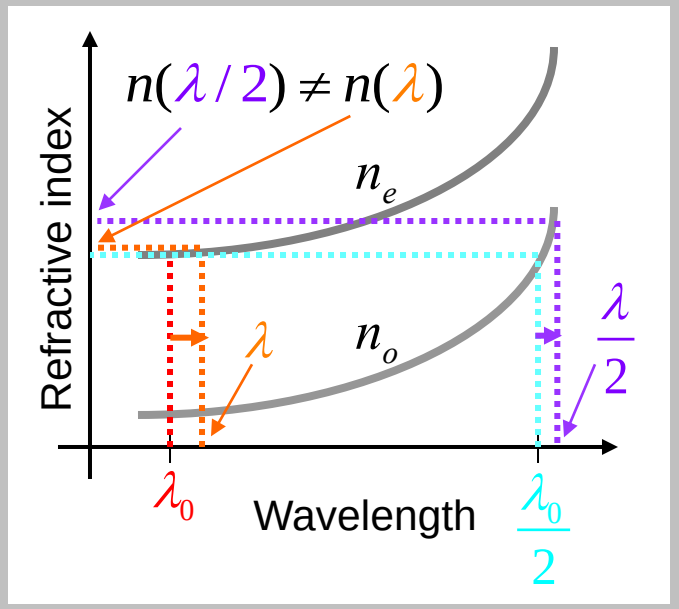

$$\Delta k(\lambda) = \frac{4\pi}{\lambda}\left[n(\lambda) - n(\lambda/2)\right]$$

Phase-matching only works exactly for one wavelength, say λ_0. Since ultrashort pulses have lots of bandwidth, achieving approximate phase-matching for all frequencies is a big issue.

The range of wavelengths (or frequencies) that achieve approximate phase-matching is the phase-matching bandwidth.

Phase-matching efficiency vs. wavelength for BBO

Phase-matching efficiency vs. wavelength for the nonlinear-optical crystal, beta-barium borate (BBO), for different crystal thicknesses:

10 μm

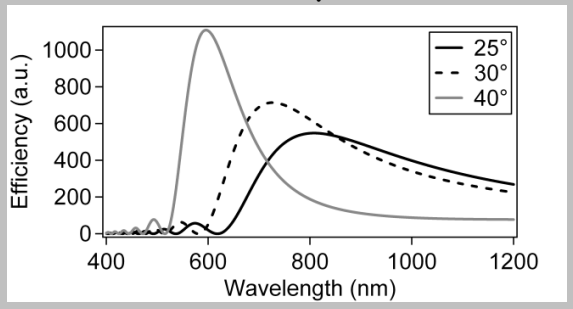

100 μm

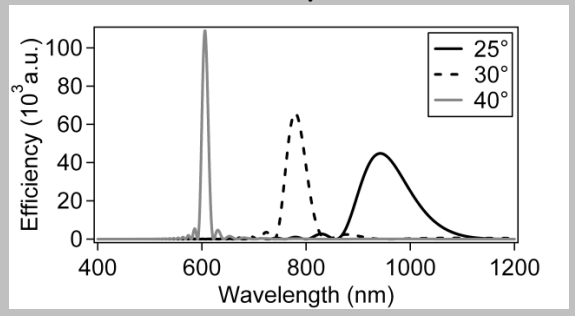

1000 μm

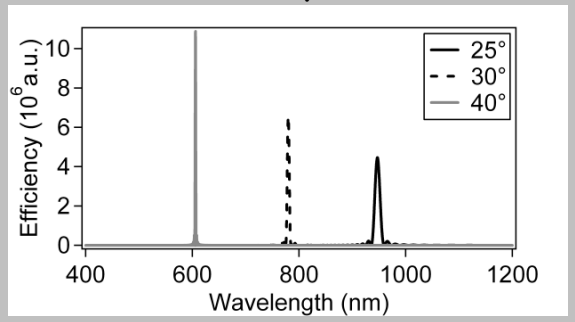

These curves also take into account the $(L/\lambda)^2$ factor.

While the curves are scaled in arbitrary units, the relative magnitudes can be compared among the three plots. (These curves don't, however, include the nonlinear susceptibility, $\chi^{(2)}$).

Note the huge differences in phase-matching bandwidth and efficiency with crystal thickness.

Phase-matching efficiency vs. wavelength for KDP

Phase-matching efficiency vs. wavelength for the nonlinear-optical crystal, potassium dihydrogen phosphate (KDP), for different crystal thicknesses:

10 μm

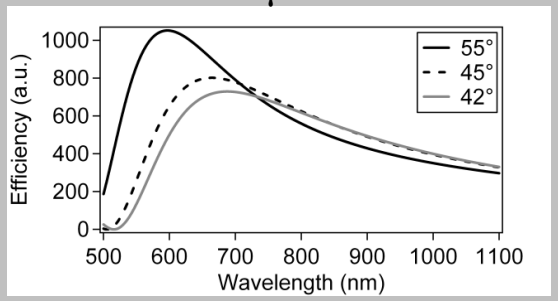

100 μm

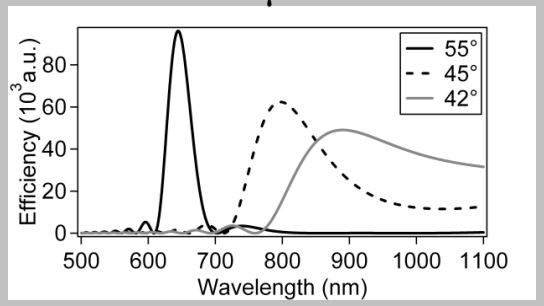

1000 μm

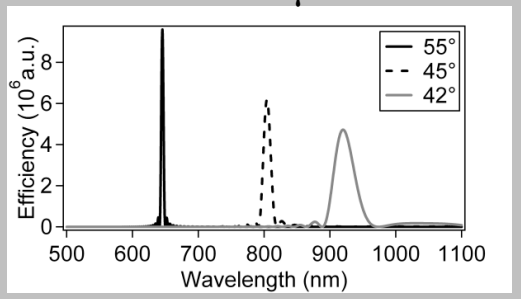

The huge differences in phase-matching bandwidth and efficiency with crystal thickness occur for all crystals.

The curves for the thin crystals don't fall to zero at long wavelengths because KDP simultaneously phase-matches for two wavelengths, that shown and a longer (IR) wavelength, whose phase-matching ranges begin to overlap when the crystal is thin.

Calculation of phase-matching bandwidth

The phase-mismatch is:

$$\Delta k(\lambda) = \frac{4\pi}{\lambda}\left[n(\lambda) - n(\lambda/2)\right]$$

Assuming the process is phase-matched at λ_0, let's see what the phase-mismatch will be at $\lambda = \lambda_0 + \delta\lambda$

But the process is phase-matched at λ_0

$$\Delta k(\lambda) = \frac{4\pi}{\lambda_0}\left[1 - \frac{\delta\lambda}{\lambda_0}\right]\left[n(\lambda_0) + \delta\lambda\, n'(\lambda_0) - n(\lambda_0/2) - \frac{\delta\lambda}{2}n'(\lambda_0/2)\right]$$

because, when the input wavelength changes by $\delta\lambda$, the second-harmonic wavelength changes by only $\delta\lambda/2$.

$$\Delta k(\lambda) = \frac{4\pi\,\delta\lambda}{\lambda_0}\left[n'(\lambda_0) - \frac{1}{2}n'(\lambda_0/2)\right]$$

to first order in $\delta\lambda$

Calculation of phase-matching bandwidth (cont'd)

The sinc^2 curve will decrease by a factor of 2 when $\Delta k\, L/2 = \pm 1.39$. So solving for the wavelength range that yields $|\Delta k| < 2.78/L$ yields the phase-matching bandwidth.

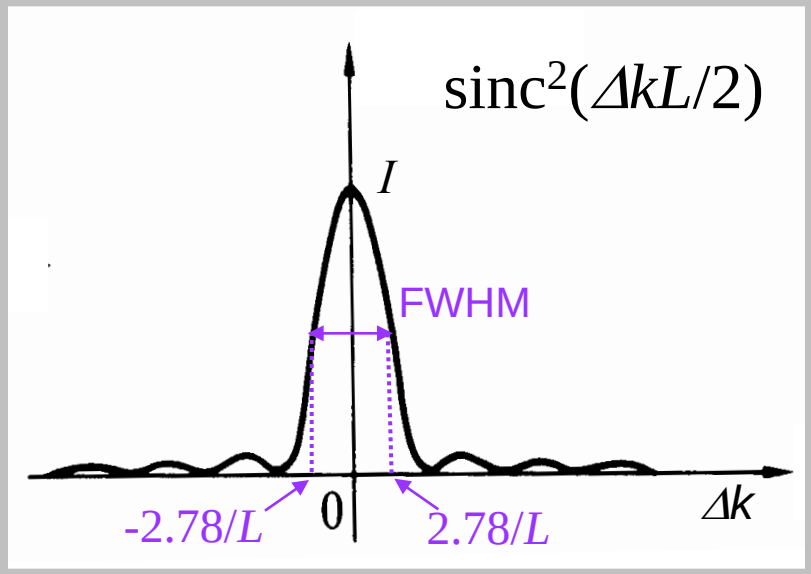

$$-2.78/L < \frac{4\pi\,\delta\lambda}{\lambda_0}\left[n'(\lambda_0) - \frac{1}{2}n'(\lambda_0/2)\right] < 2.78/L$$

$$\delta\lambda_{FWHM} = \frac{0.44\,\lambda_0/L}{\left|n'(\lambda_0) - \frac{1}{2}n'(\lambda_0/2)\right|}$$

Phase-matching bandwidth: BBO & KDP

The phase-matching bandwidth is usually too small, but it increases as the crystal gets thinner or the dispersion decreases (i.e., the wavelength approaches ~1.5 microns for typical media).

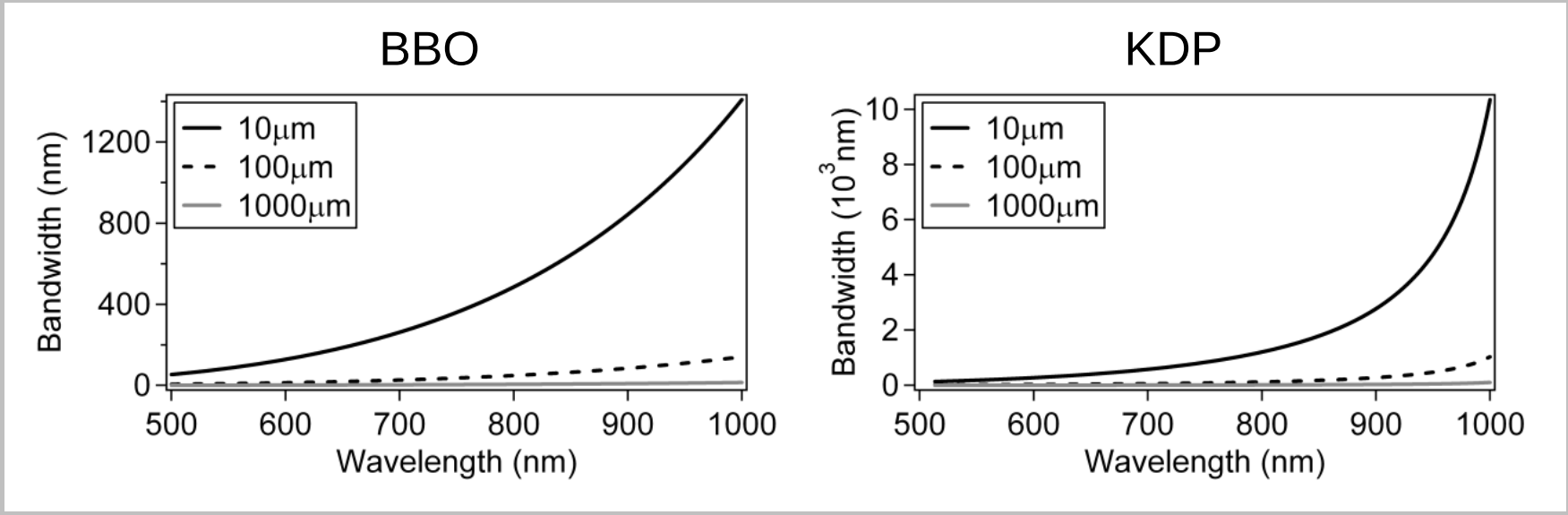

The theory breaks down, however, when the bandwidth approaches the wavelength.

Group-velocity mismatch

Inside the crystal the two different wavelengths have different group velocities.

Define the Group-Velocity Mismatch (GVM):

$$GVM \equiv \frac{1}{v_g(\lambda_0/2)} - \frac{1}{v_g(\lambda_0)}$$

As the pulse enters the crystal:

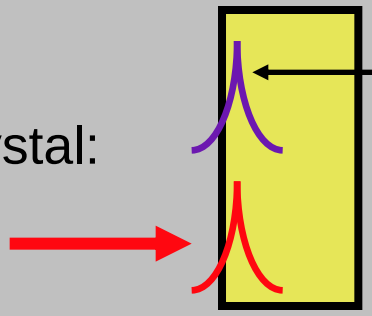

Second harmonic created just as pulse enters crystal (overlaps the input pulse)

Crystal

As the pulse leaves the crystal:

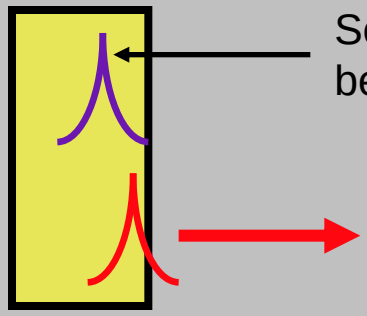

Second harmonic pulse lags behind input pulse due to GVM

Group-velocity mismatch

Calculating GVM:

$$v_g(\lambda) = \frac{c_0 / n(\lambda)}{1 - \frac{\lambda}{n(\lambda)} n'(\lambda)} \qquad \text{So:} \quad \frac{1}{v_g(\lambda)} = \frac{n(\lambda)}{c_0}\left[1 - \frac{\lambda}{n(\lambda)} n'(\lambda)\right]$$

$$GVM \equiv \frac{1}{v_g(\lambda_0/2)} - \frac{1}{v_g(\lambda_0)}$$

$$= \frac{n(\lambda_0/2)}{c_0}\left[1 - \frac{\lambda_0/2}{n(\lambda_0/2)} n'(\lambda_0/2)\right] - \frac{n(\lambda_0)}{c_0}\left[1 - \frac{\lambda_0}{n(\lambda_0)} n'(\lambda_0)\right]$$

But we only care about GVM when $n(\lambda_0/2) = n(\lambda_0)$

$$GVM = \frac{\lambda_0}{c_0}\left[n'(\lambda_0) - \frac{1}{2} n'(\lambda_0/2)\right]$$

Group-velocity mismatch lengthens the SH pulse.

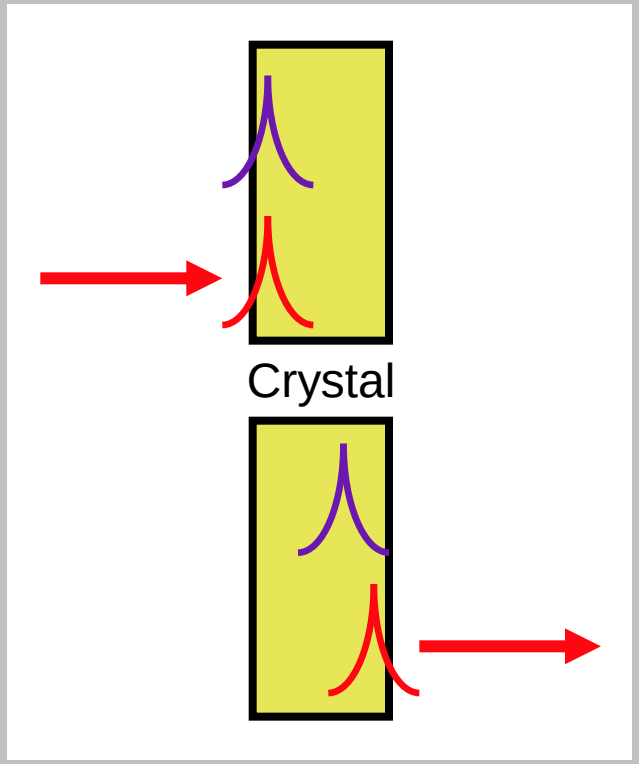

Assuming that a very short pulse enters the crystal, the length of the SH pulse, δt, will be determined by the difference in light-travel times through the crystal:

$$\delta t = \frac{L}{v_g(\lambda_0/2)} - \frac{L}{v_g(\lambda_0)} = L\ GVM$$

We always try to satisfy: $L\ GVM << \tau_p$

Group-velocity mismatch pulse lengthening

Second-harmonic pulse shape for different crystal lengths:

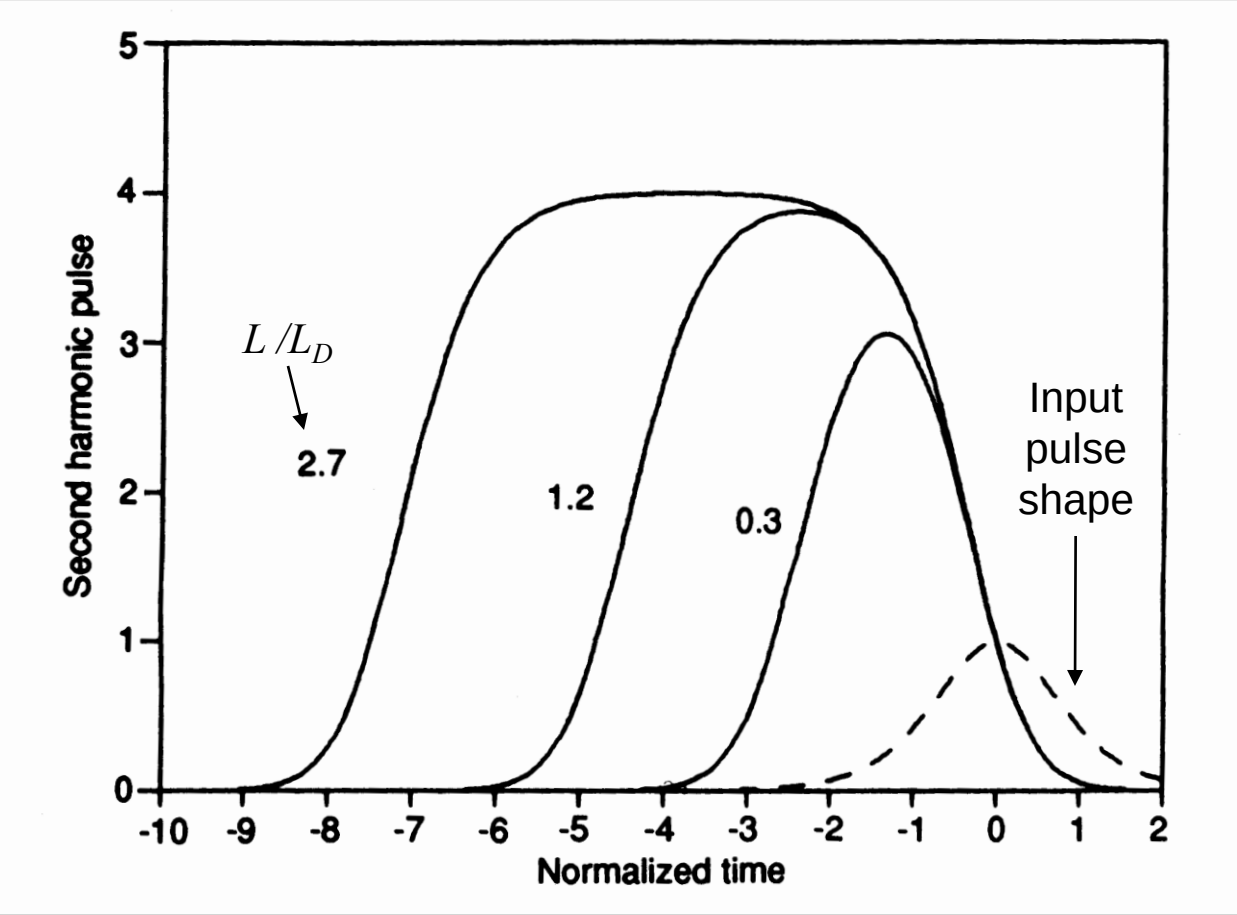

$$L_D \equiv \frac{\tau_p}{GVM}$$

L_D is the crystal length that doubles the pulse length.

It's best to use a very thin crystal. Sub-100-micron crystals are common.

Group-velocity mismatch numbers

crystal	λ [nm]	θ [°]	$(v_2^{-1} - v_1^{-1})$ [fs/mm]
KDP	550	71	266
	620	58	187
	800	45	77
	1000	41	9
$LiIO_3$	620	61	920
	800	42	513
	1000	32	312
BBO	500	52	680
	620	40	365
	800	30	187
	1000	24	100
	1500	20	5

Group-velocity mismatch limits bandwidth.

Let's compute the second-harmonic bandwidth due to GVM.

Take the SH pulse to have a Gaussian intensity, for which $\delta t\ \delta\nu = 0.44$. Rewriting in terms of the wavelength,

$$\delta t\ \delta\lambda = \delta t\ \delta\nu\,[d\nu/d\lambda]^{-1} = 0.44\,[d\nu/d\lambda]^{-1} = 0.44\ \lambda^2/c_0$$

where we've neglected the minus sign since we're computing the bandwidth, which is inherently positive. So the bandwidth is:

$$\delta\lambda_{FWHM} \approx \frac{0.44\,\lambda_0^2/c_0}{\delta t} = \frac{0.44\,\lambda_0^2/c_0}{L\ GVM}$$

$$GVM = \frac{\lambda_0}{c_0}\left[n'(\lambda_0) - \frac{1}{2}n'(\lambda_0/2)\right]$$

$$\boxed{\delta\lambda_{FWHM} \approx \frac{0.44\,\lambda_0/L}{\left|n'(\lambda_0) - \frac{1}{2}n'(\lambda_0/2)\right|}}$$

Calculating the bandwidth by considering the GVM yields the same result as the phase-matching bandwidth!

Alternative method for phase-matching: periodic poling

Recall that the second-harmonic phase alternates every coherence length when phase-matching is not achieved, which is always the case for the same polarizations—whose nonlinearity is much higher.

Periodic poling solves this problem. But such complex crystals are hard to grow and have only recently become available.

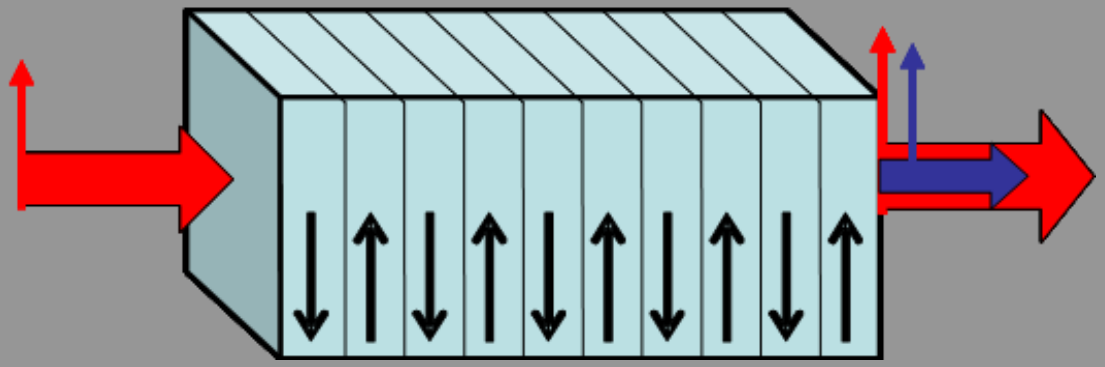

Periodically Poled Lithium Niobate (PPLN)

SHG efficiency (rough estimation)

The second-harmonic field is given by:

$$E^{2\omega}(L,t) = -i\frac{\mu_0\omega^2 L}{2k} P \exp(i\Delta kL/2)\,\mathrm{sinc}(\Delta kL/2)$$

The irradiance will be:

$$I^{2\omega} = \frac{\eta_0\omega^2(\chi^{(2)})^2(I^{\omega})^2 L^2}{2{c_0}^2 n^3}\,\mathrm{sinc}^2(\Delta kL/2)$$

Dividing by the input irradiance to obtain the SHG efficiency:

$$\frac{I^{2\omega}}{I^{\omega}} = \frac{2\eta_0\omega^2 d^2 I^{\omega} L^2}{{c_0}^2 n^3}$$

Take $\Delta k = 0$

$d \propto \chi^{(2)}$, and includes crystal additional parameters.

Substituting in typical numbers:

$$\frac{I^{2\omega}}{I^{\omega}} \approx [5\times10^{-8}/W]\; I^{\omega}\; L^2$$

Serious second-harmonic generation

Frequency-doubling KDP crystals at Lawrence Livermore National Laboratory

These crystals convert as much as 80% of the input light to its second harmonic. Then additional crystals produce the third harmonic with similar efficiency!

These guys are serious!

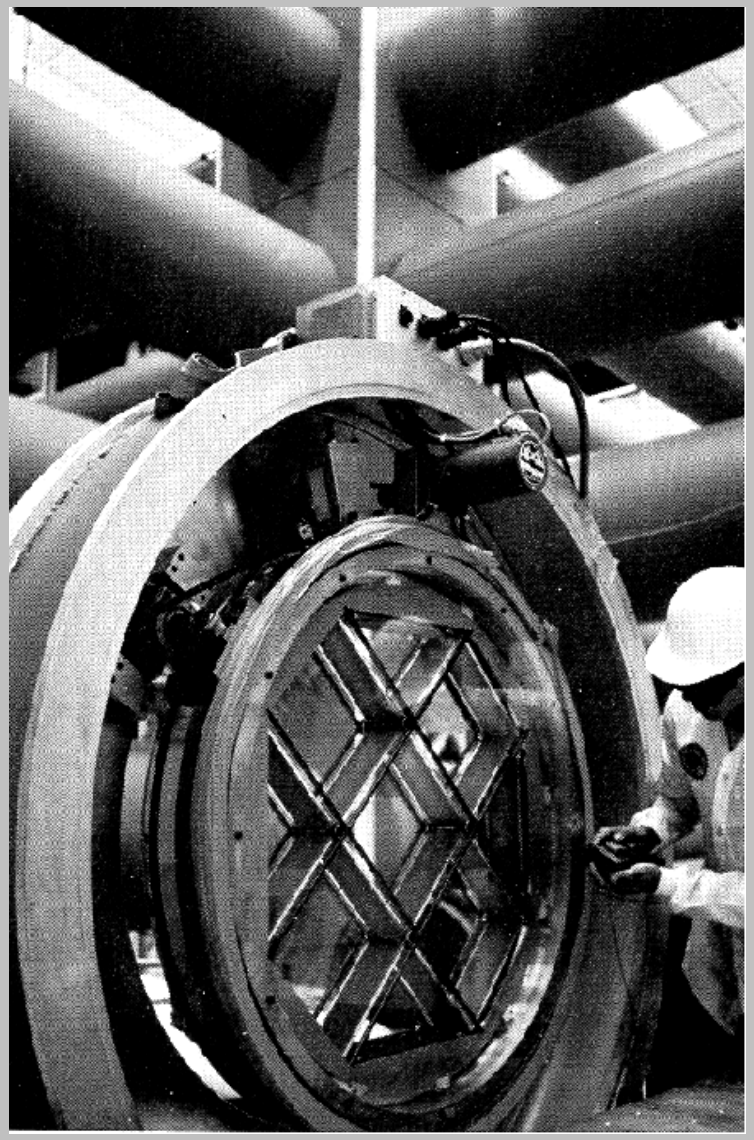

Third harmonic generation via 2nd order nonlinearities

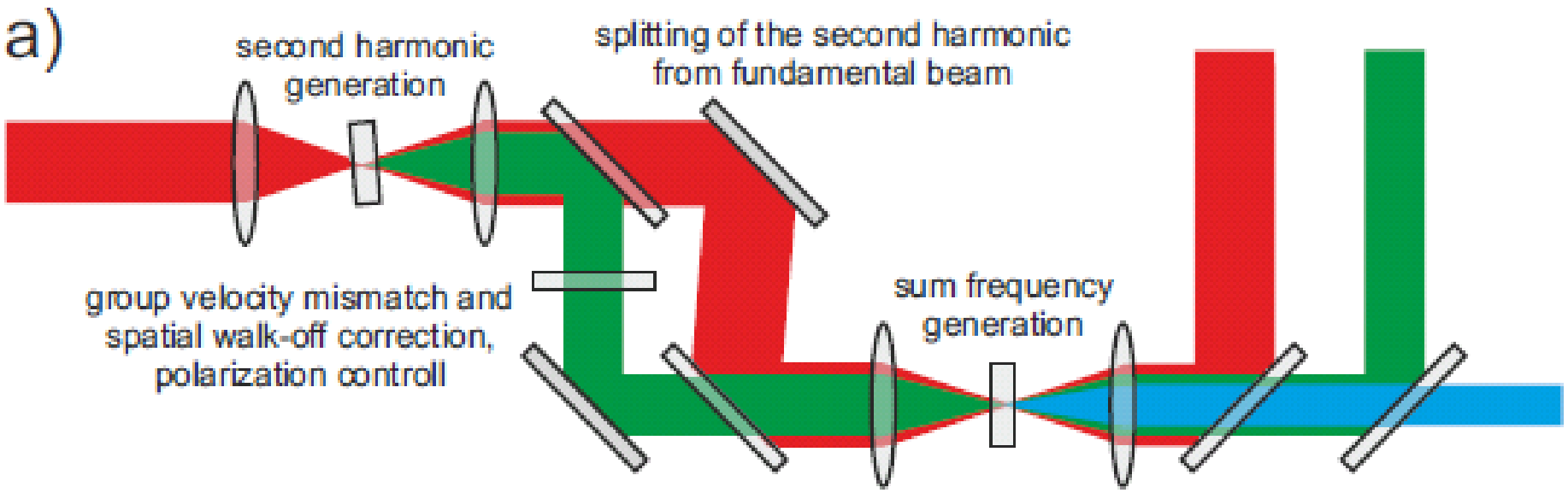

Third harmonic generation via 2nd order nonlinearities

The pulses must overlap in time and in space

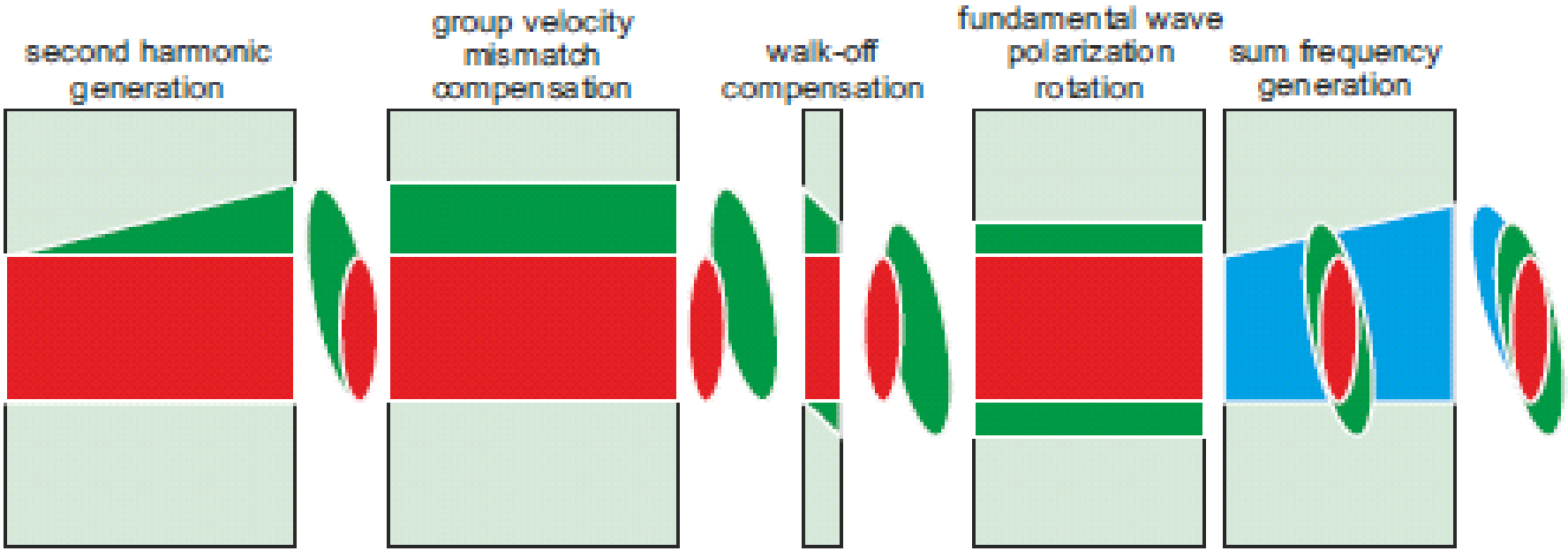

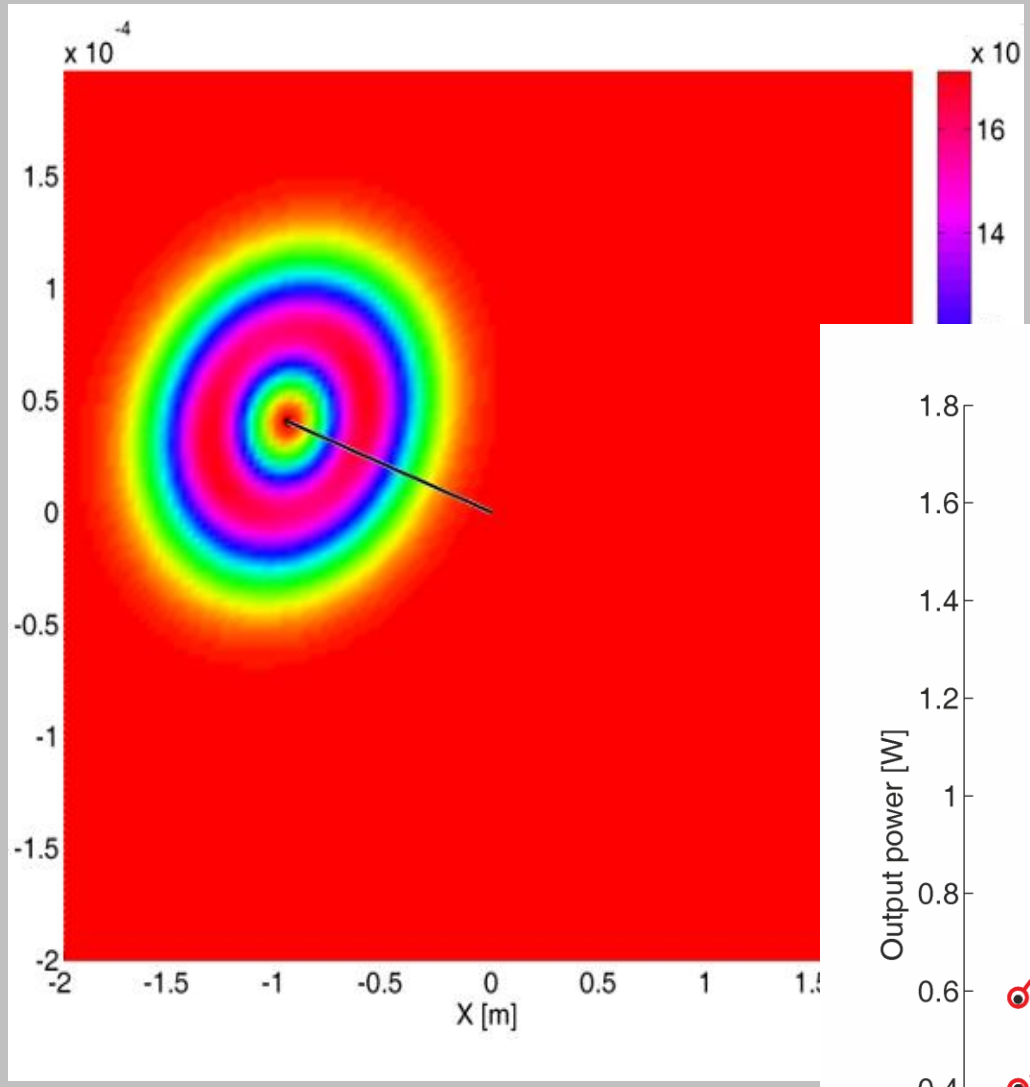
x 10^-4
x 10
16
14
1.5
1
0.5
0
-0.5
-1
-1.5
-2
-2
-1.5
-1
-0.5
0
0.5
1
X [m]

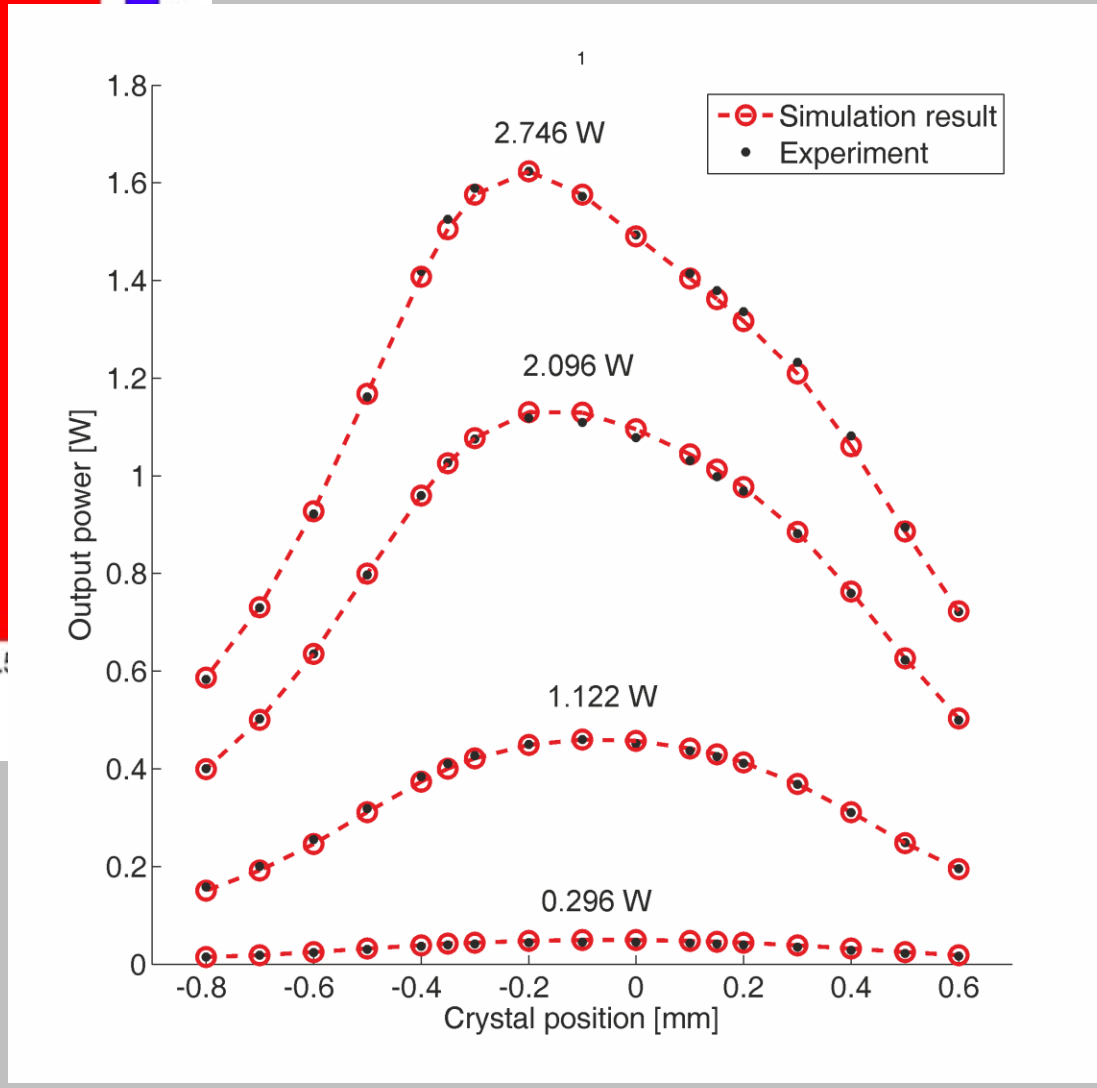
1
Simulation result
Experiment
2.746 W
2.096 W
1.122 W
0.296 W
Output power [W]
1.8
1.6
1.4
1.2
1
0.8
0.6
0.4
0.2
0
-0.8
-0.6
-0.4
-0.2
0
0.2
0.4
0.6
Crystal position [mm]

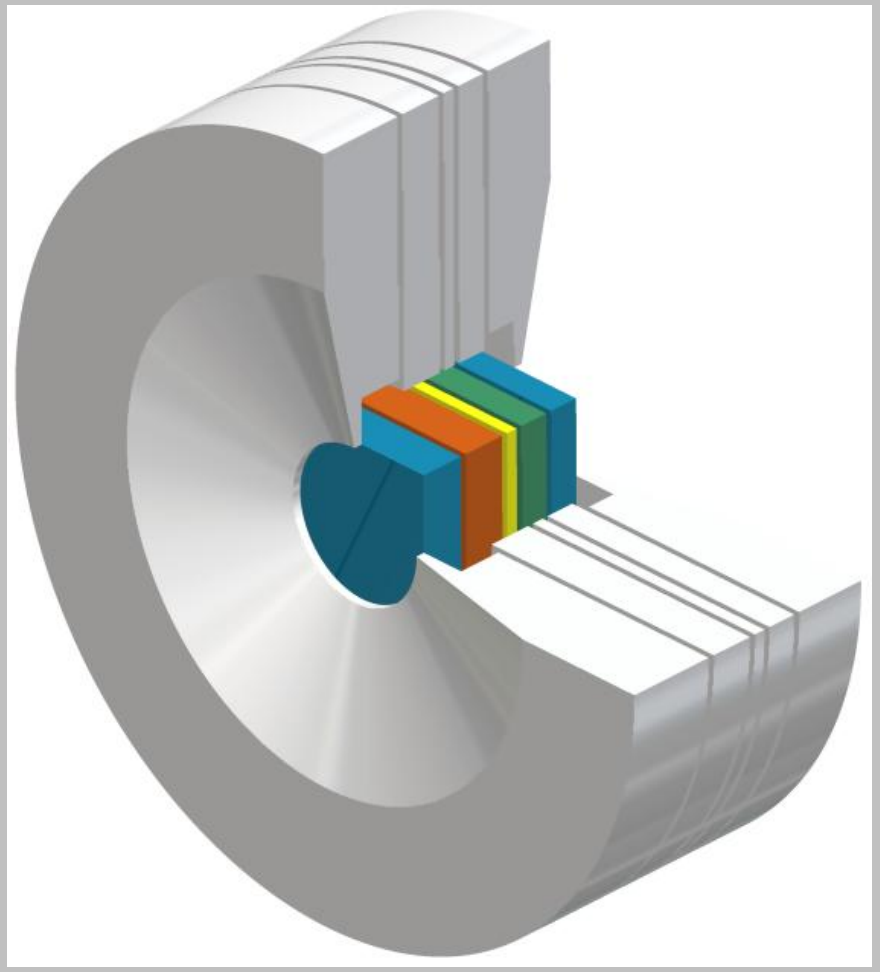

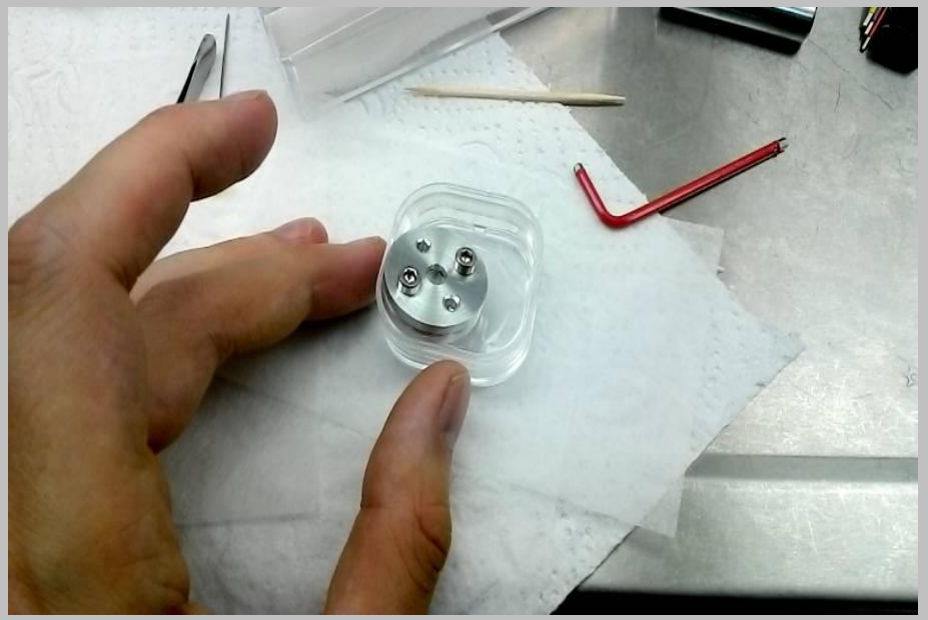

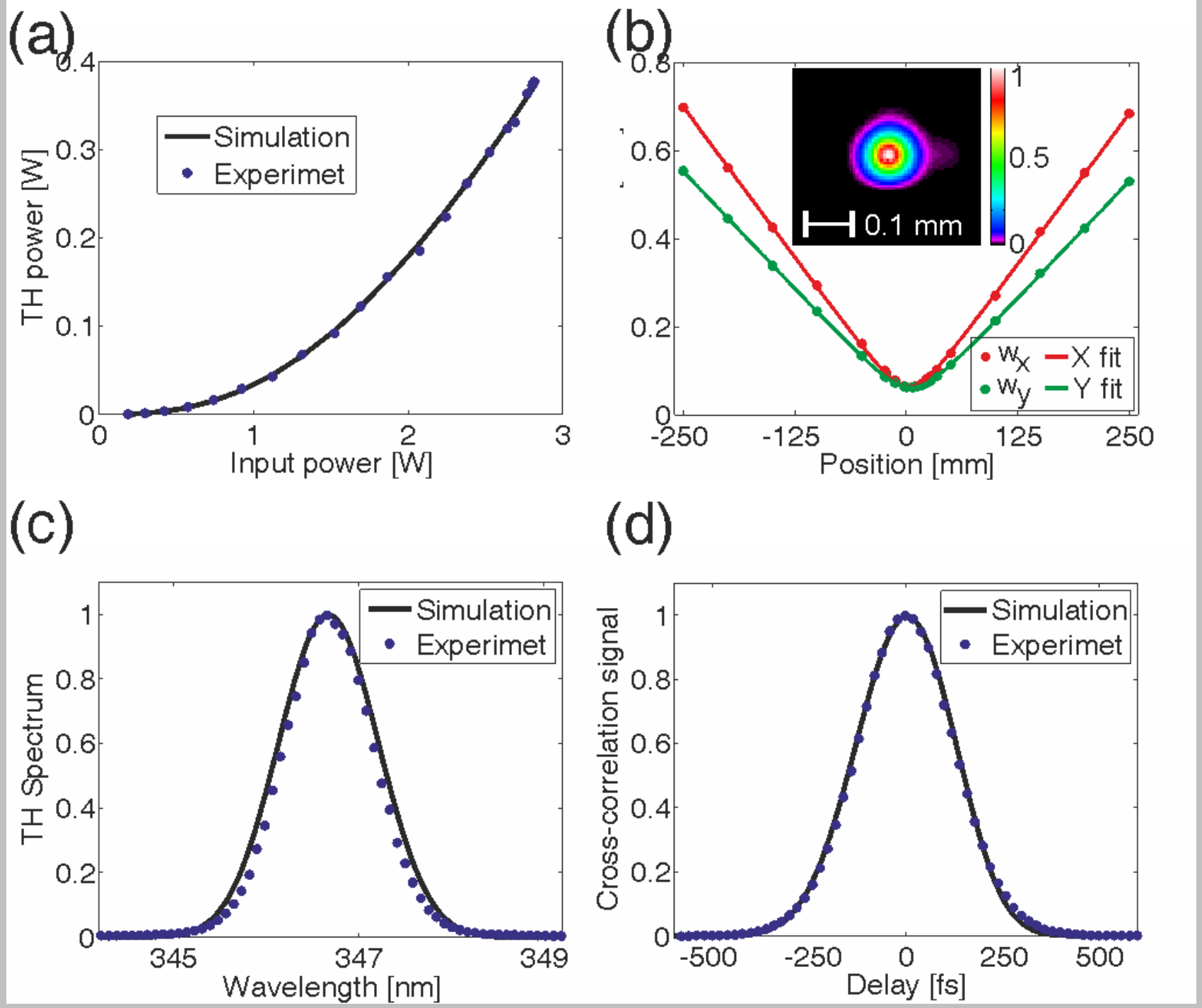
(a)
TH power [W]
Input power [W]
Simulation
Experimet
0
0.1
0.2
0.3
0.4
0
1
2
3
(b)
Position [mm]
0.1 mm
1
0.5
0
w_x
X fit
w_y
Y fit
0
0.2
0.4
0.6
0.8
-250
-125
0
125
250
(c)
TH Spectrum
Wavelength [nm]
Simulation
Experimet
0
0.2
0.4
0.6
0.8
1
345
347
349
(d)
Cross-correlation signal
Delay [fs]
Simulation
Experimet
0
0.2
0.4
0.6
0.8
1
-500
-250
0
250
500

Difference-Frequency Generation: Optical Parametric Generation, Amplification, Oscillation

Difference-frequency generation takes many useful forms.

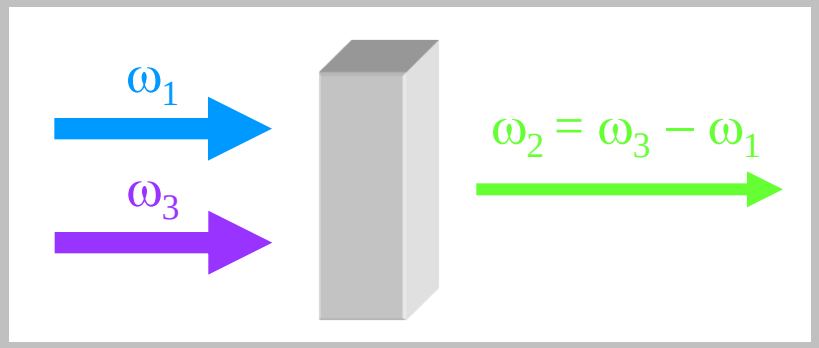

Parametric Down-Conversion
(Difference-frequency generation)

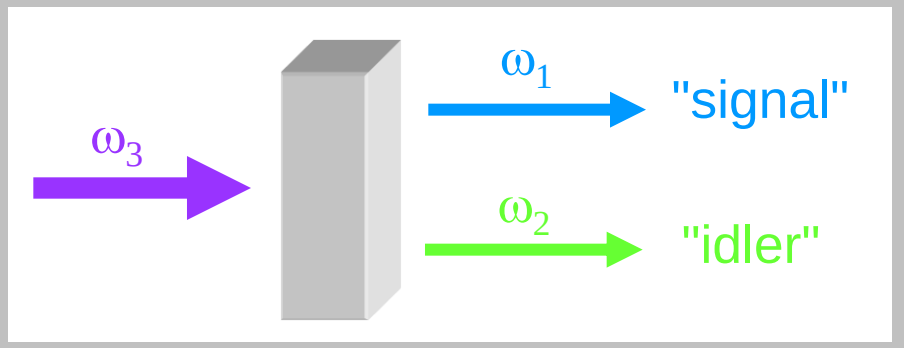

Optical Parametric
Generation (OPG)

By convention:
$\omega_{signal} > \omega_{idler}$

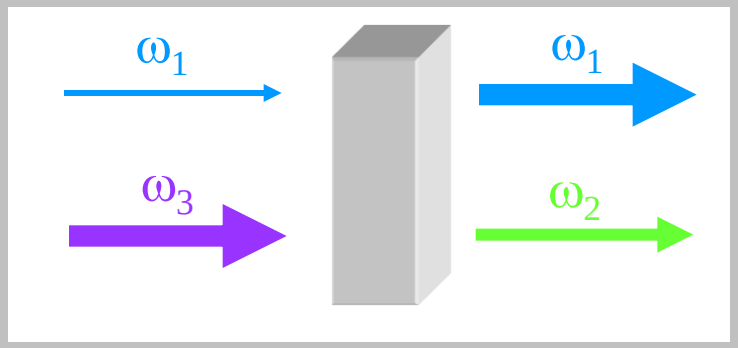

Optical Parametric
Amplification (OPA)

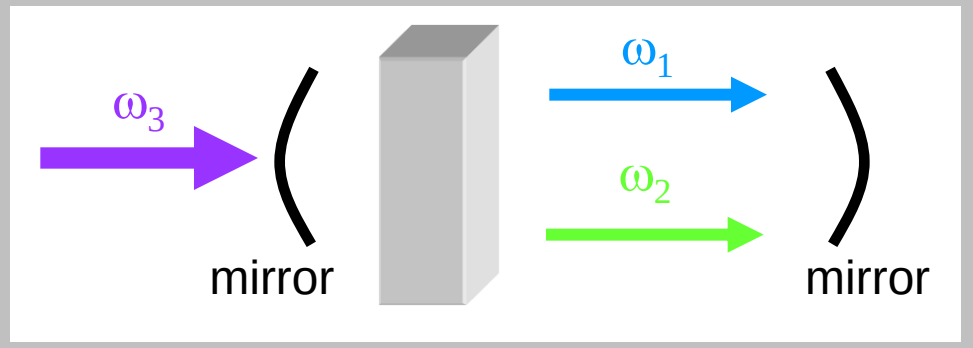

Optical Parametric
Oscillation (OPO)

Optical Parametric Generation

Equations are just about identical to those for SHG:

$$\left(\frac{\partial}{\partial z}+\frac{1}{v_{g1}}\frac{\partial}{\partial t}\right)E_1=-i\chi^{(2)}\frac{\omega_1^2}{2c^2k_1}E_2^*E_3e^{i\Delta k\cdot z}$$

$$\left(\frac{\partial}{\partial z}+\frac{1}{v_{g2}}\frac{\partial}{\partial t}\right)E_2=-i\chi^{(2)}\frac{\omega_2^2}{2c^2k_2}E_1^*E_3e^{i\Delta k\cdot z}$$

$$\left(\frac{\partial}{\partial z}+\frac{1}{v_{g3}}\frac{\partial}{\partial t}\right)E_3=-i\chi^{(2)}\frac{\omega_3^2}{2c^2k_3}E_1E_2e^{-i\Delta k\cdot z}$$

where:

k_i = wave vector of i^{th} wave

$\Delta k = k_1 + k_2 - k_3$

v_{gi} = group velocity of i^{th} wave

The solutions for E_1 and E_2 involve exponential gain!

OPA's etc. are ideal uses of ultrashort pulses, whose intensities are high.

Phase-matching applies.

We can vary the crystal angle in the usual manner, or we can vary the crystal temperature (since n depends on T).

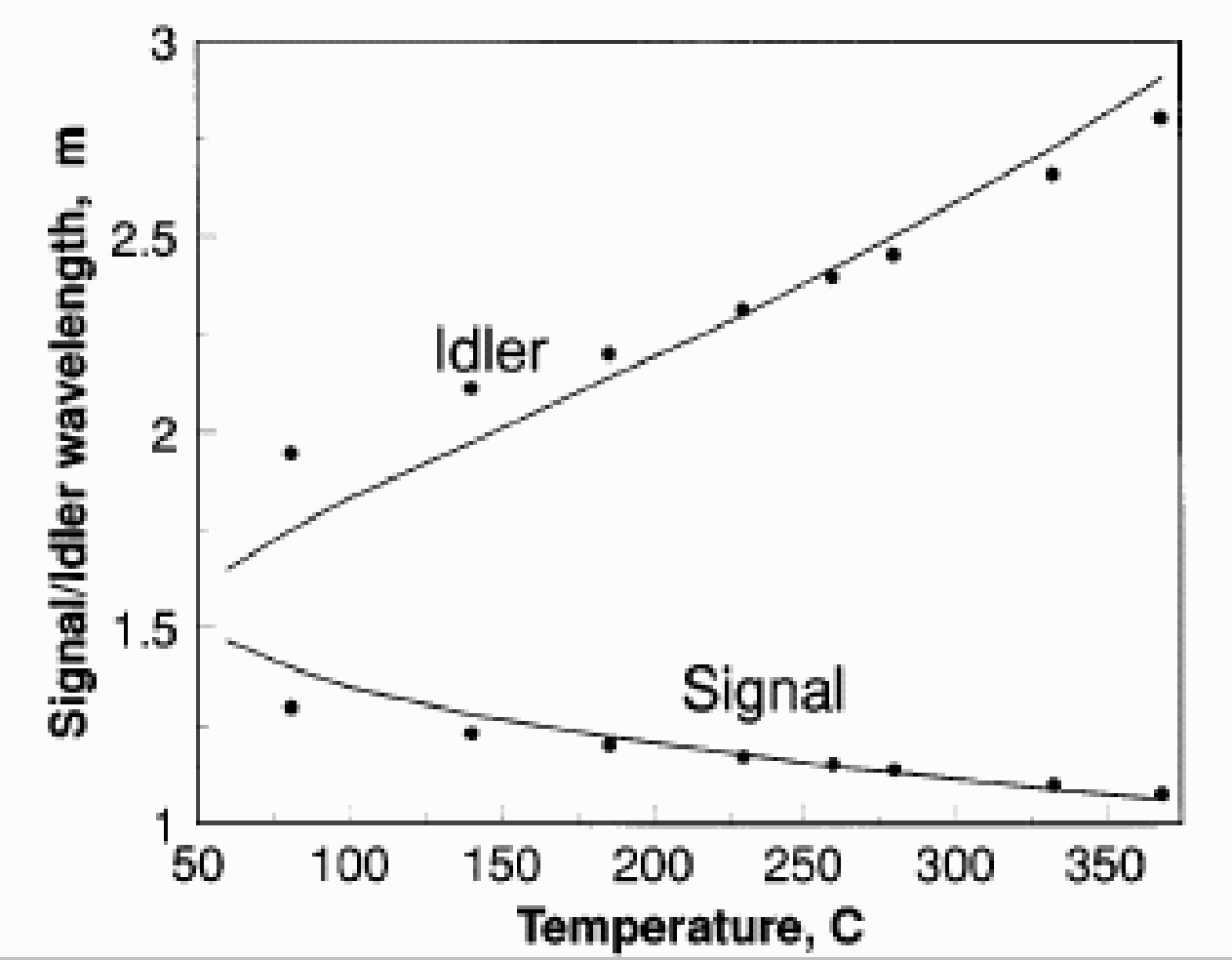

Free code to perform OPO, OPA, and OPG calculations

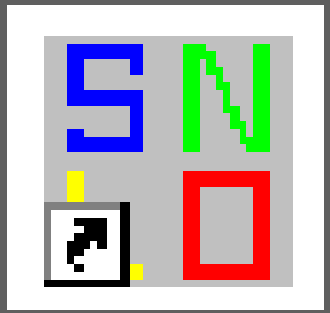

Public domain software maintained by Arlee Smith at Sandia National Labs. Just web-search ‘SNLO’.

You can use it to select the best nonlinear crystal for your particular application or perform detailed simulations of nonlinear mixing processes in crystals.

Functions in SNLO:

1. Crystal properties
2. Modeling of nonlinear crystals in various applications.
3. Designing of stable cavities, computing Gaussian focus parameters and displaying the help file.

Optical Parametric Generation

signal:

Recent results using the nonlinear medium, periodically poled $RbTiOAsO_4$

idler:

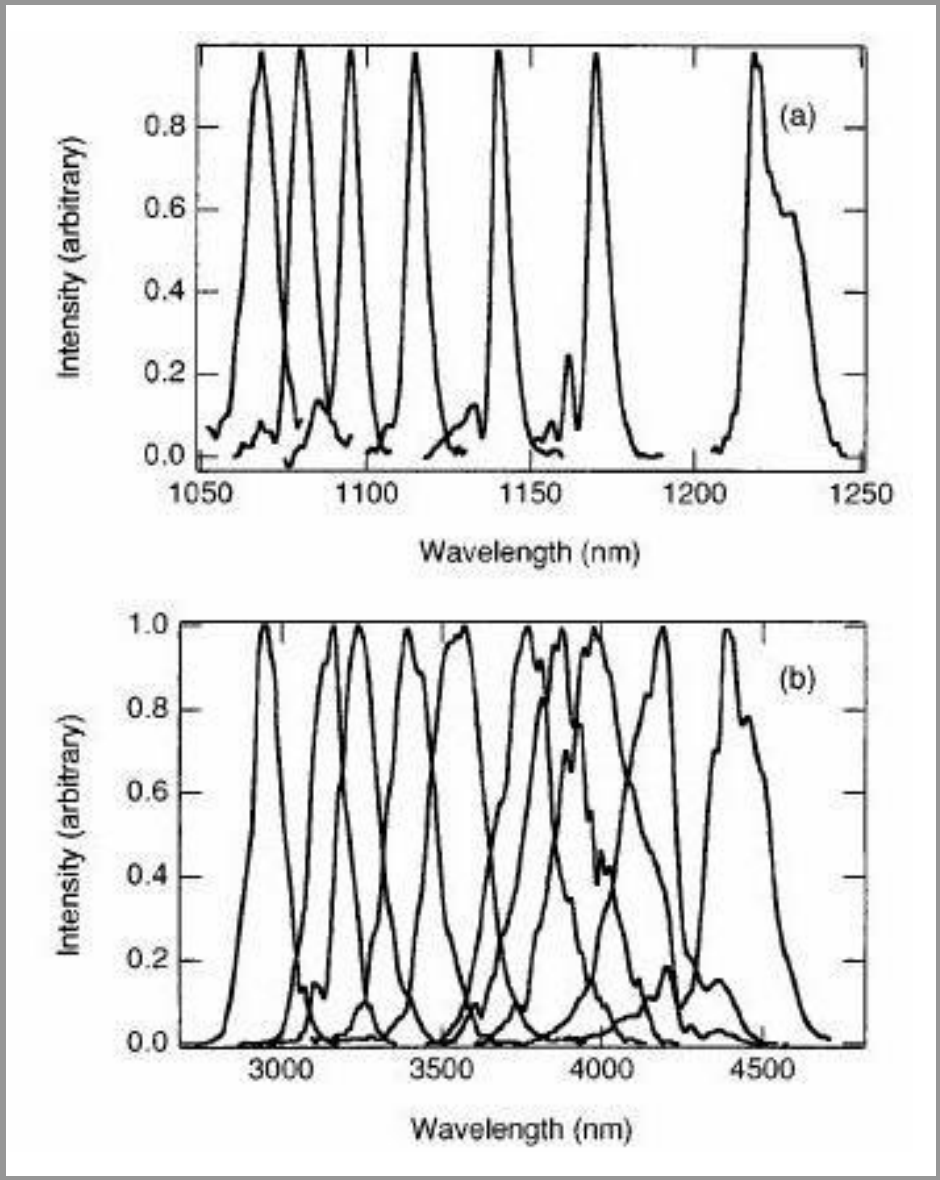

Sibbett, et al., Opt. Lett., **22**, 1397 (1997).

An ultrafast noncol-linear OPA (NOPA)

LIGHT CONVERSION

Continuum generates an arbitrary-color seed pulse.

TOPAS-white

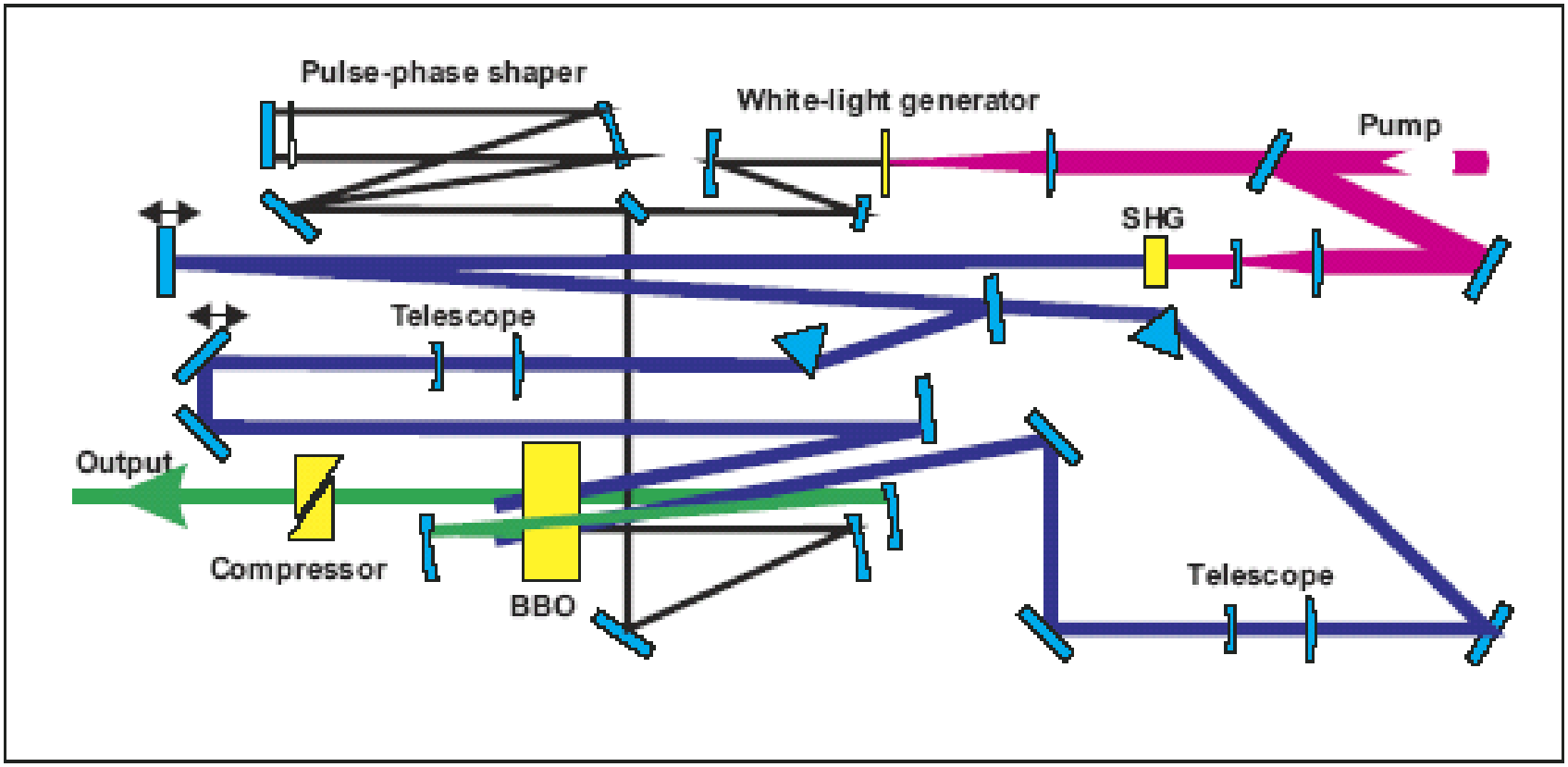

NOPA specs

LIGHT CONVERSION

TOPAS-white

Modification	Tuning ranges (nm)	
TOPAS-white	490-750, 850-1000	(Signal)
TOPAS-white-SH	245-375, 425-490	(SH of Signal)
	490-750, 850-1000	(Signal)
TOPAS-white-IR	490-750	(Signal)
	850-1700	(Idler)
TOPAS-white-IR-SH	245-375	(SH of Signal)
	425-490	(SH of Idler)
	490-750	(Signal)
	700-850	(SH of Idler)
	850-1700	(Idler)

PERFORMANCE SPECIFICATIONS WITH 0.5 mJ PUMP PULSES

SIGNAL OUTPUT (all modifications)

Tuning range	490 - 750 nm 850 - 1000 nm
Pulse energy	$\geq$ 30 μJ @ 550 nm $\geq$ 20 μJ @ 700 nm
Pulse duration, $sech^2$	$\leq$ 20 fs @ 530 - 720 nm $\leq$ 60 fs @ 490 - 530 nm $\leq$ 60 fs @ 720 - 1000 nm
Energy instability	$\leq$ 1.5% rms - 5% rms (depending on the wavelength and the input stability)
Instability of pulse duration	$\leq$ 2% rms
Pre-pulse contrast	$\leq 10^{-3}$
Spatial profile	Super-gaussian, $M^2 \leq 1.5$

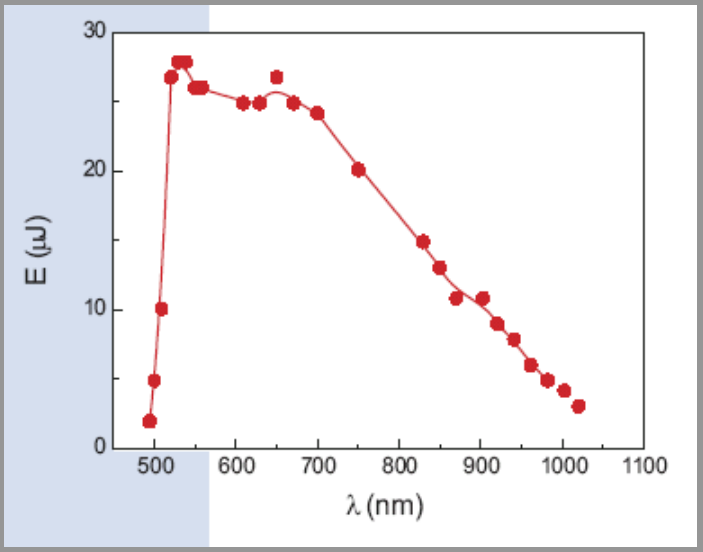

Crystals for far-IR generation

With unusual crystals, such as $AgGaS_2$, $AgGaSe_2$ or GaSe, one can obtain radiation to wavelengths as long as 20 μm.

These long wavelengths are useful for vibrational spectroscopy.

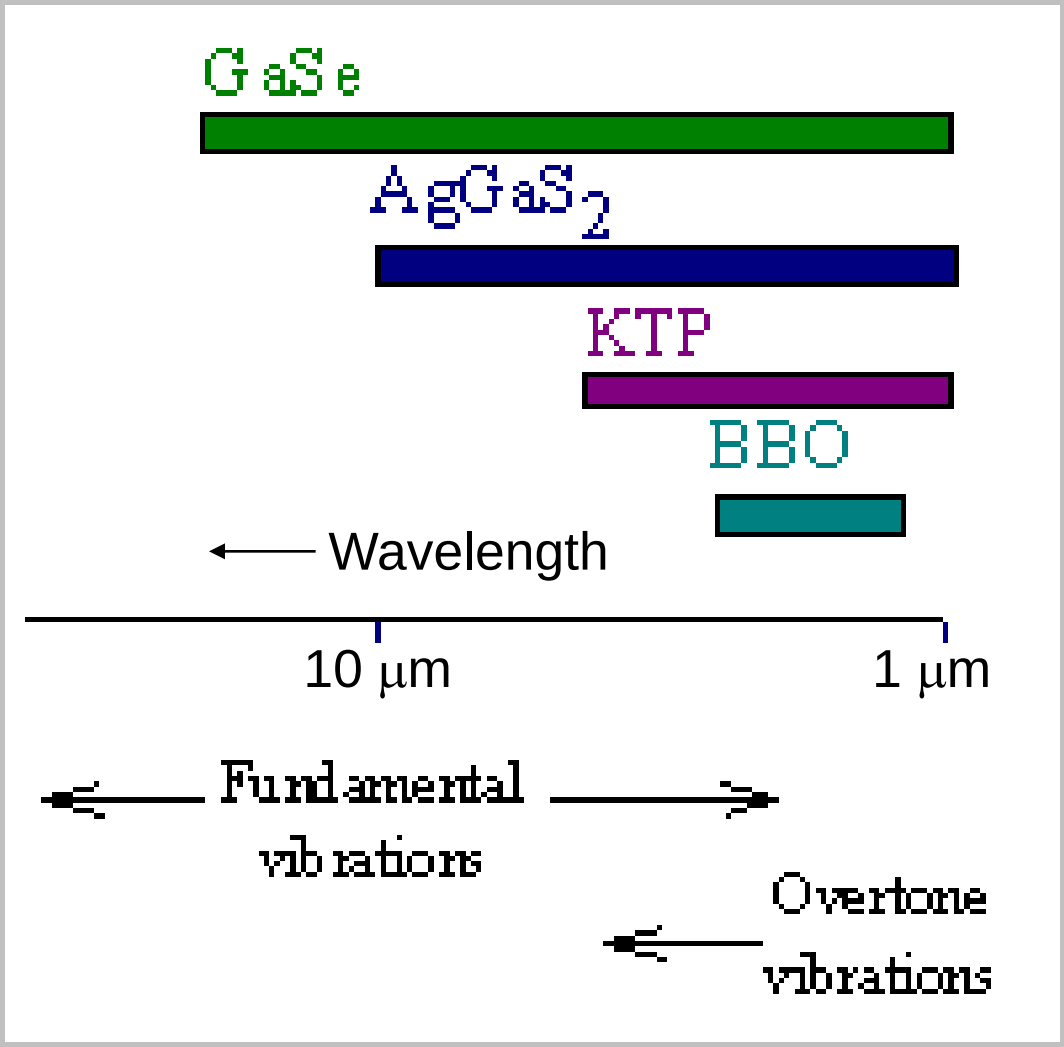

Gavin D. Reid, University of Leeds, and Klaas Wynne, University of Strathclyde

Difference-frequency generation in GaSe

Angle-tuned wavelength

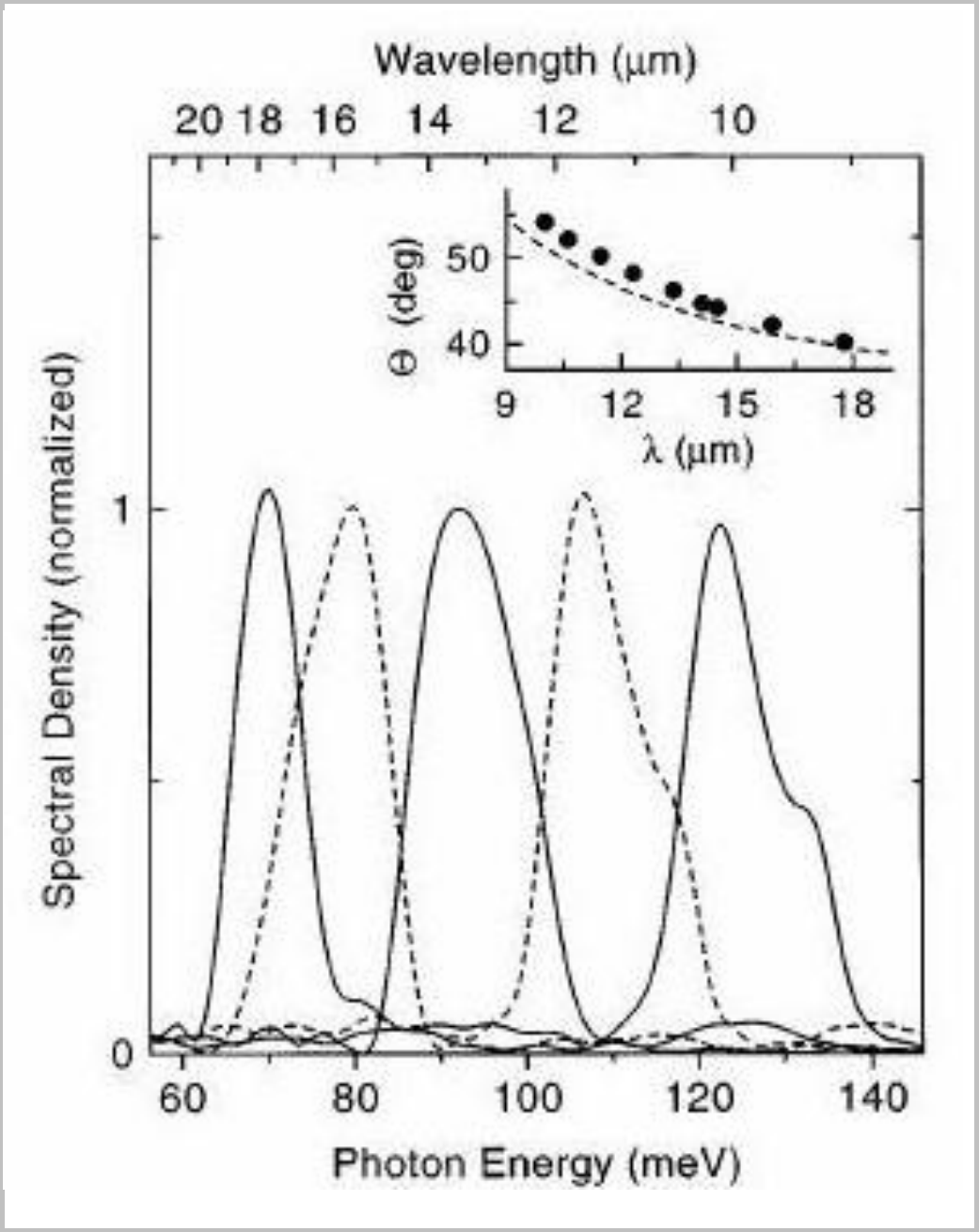

Elsaesser, et al., *Opt. Lett.*, **23**, 861 (1998)

Third-order nonlinear optical effects – supercontinuum generation (in photonic fibers)

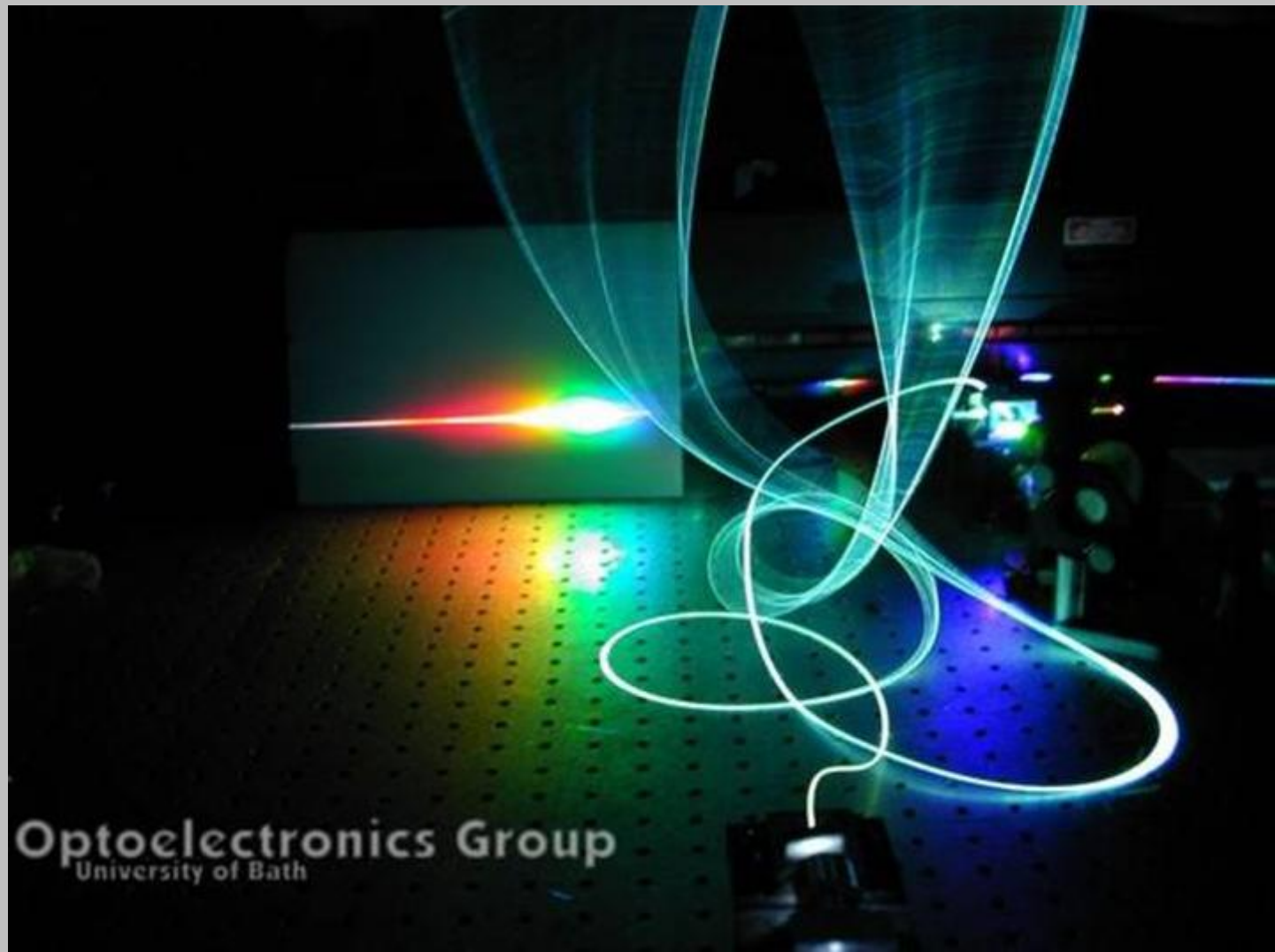

GVD in optical fibers

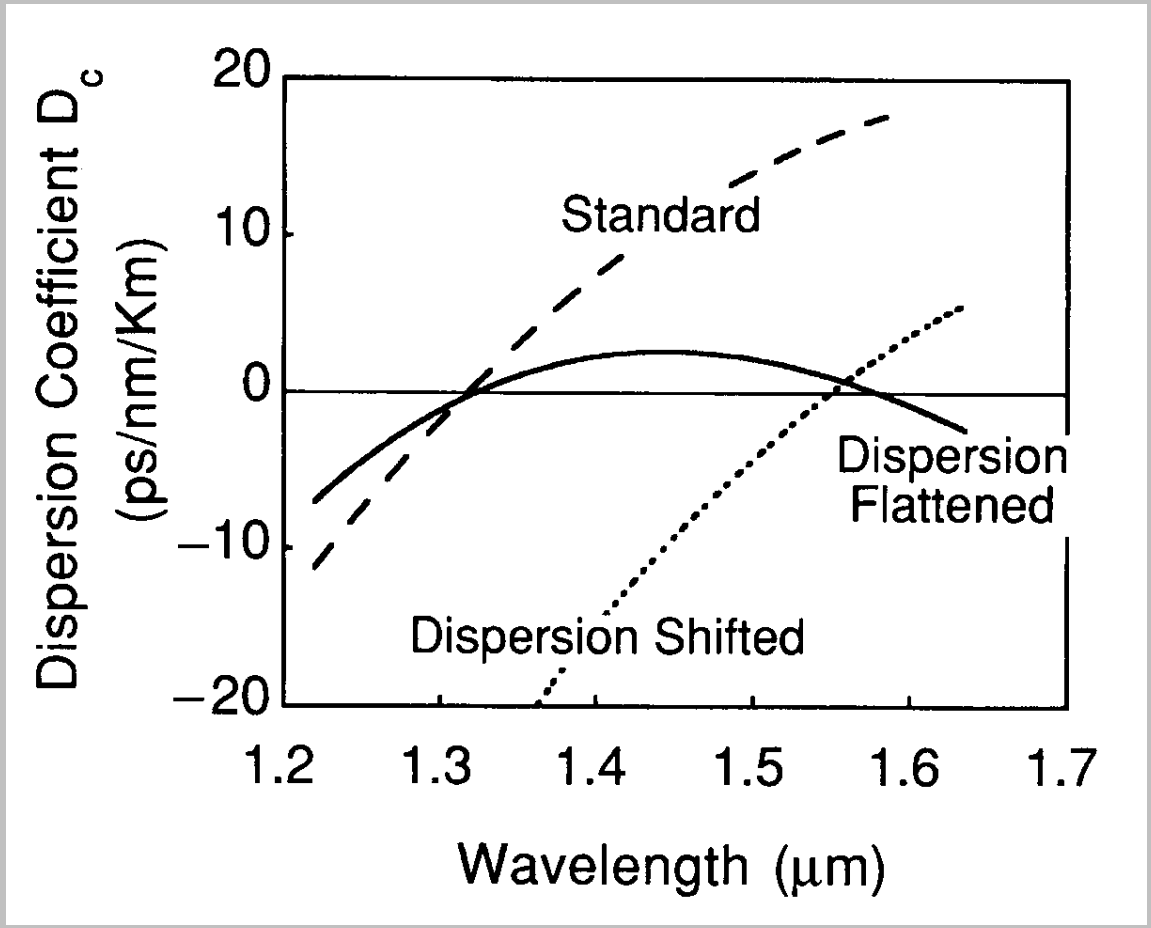

Sophisticated cladding structures, i.e., index profiles, have been designed and optimized to produce a waveguide dispersion that modifies the bulk material dispersion

Microstructured optical fibers – more degrees of freedom available at last

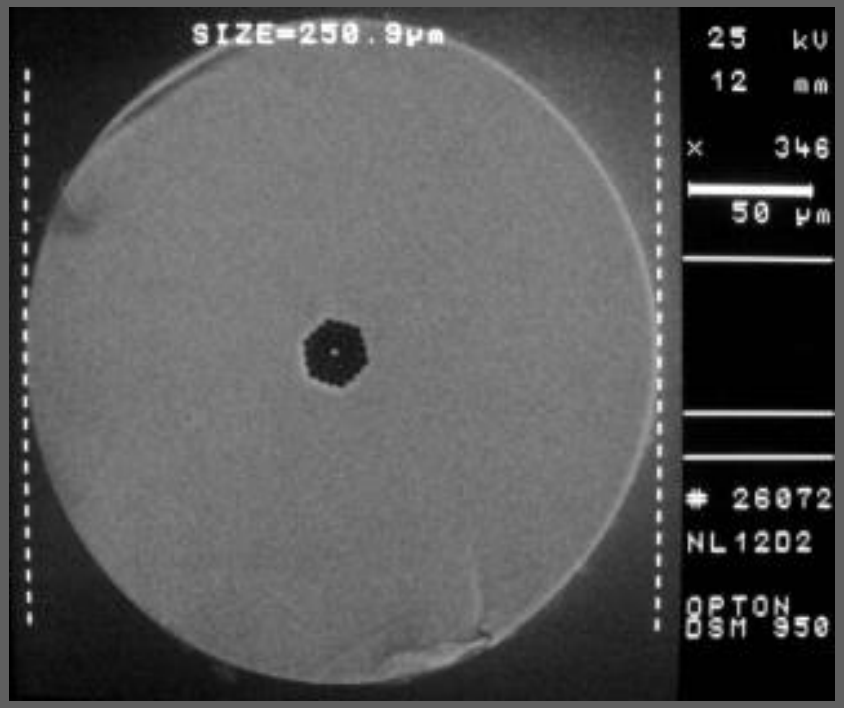

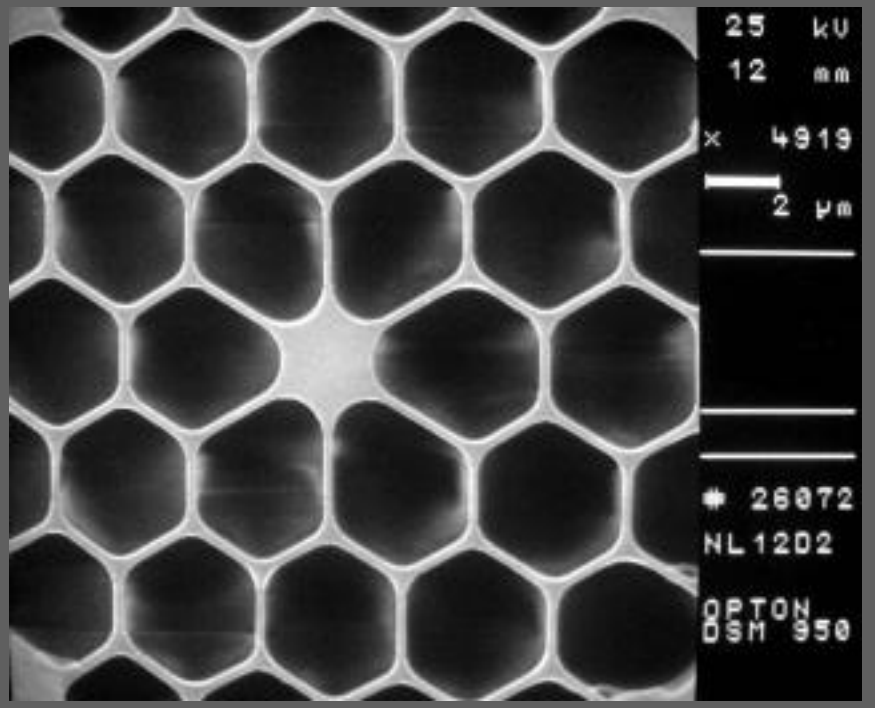

The following materials courtesy Ryszard Buczyński, IGF, FUW

Why supercontinuum?

How much light can you get into a fiber?

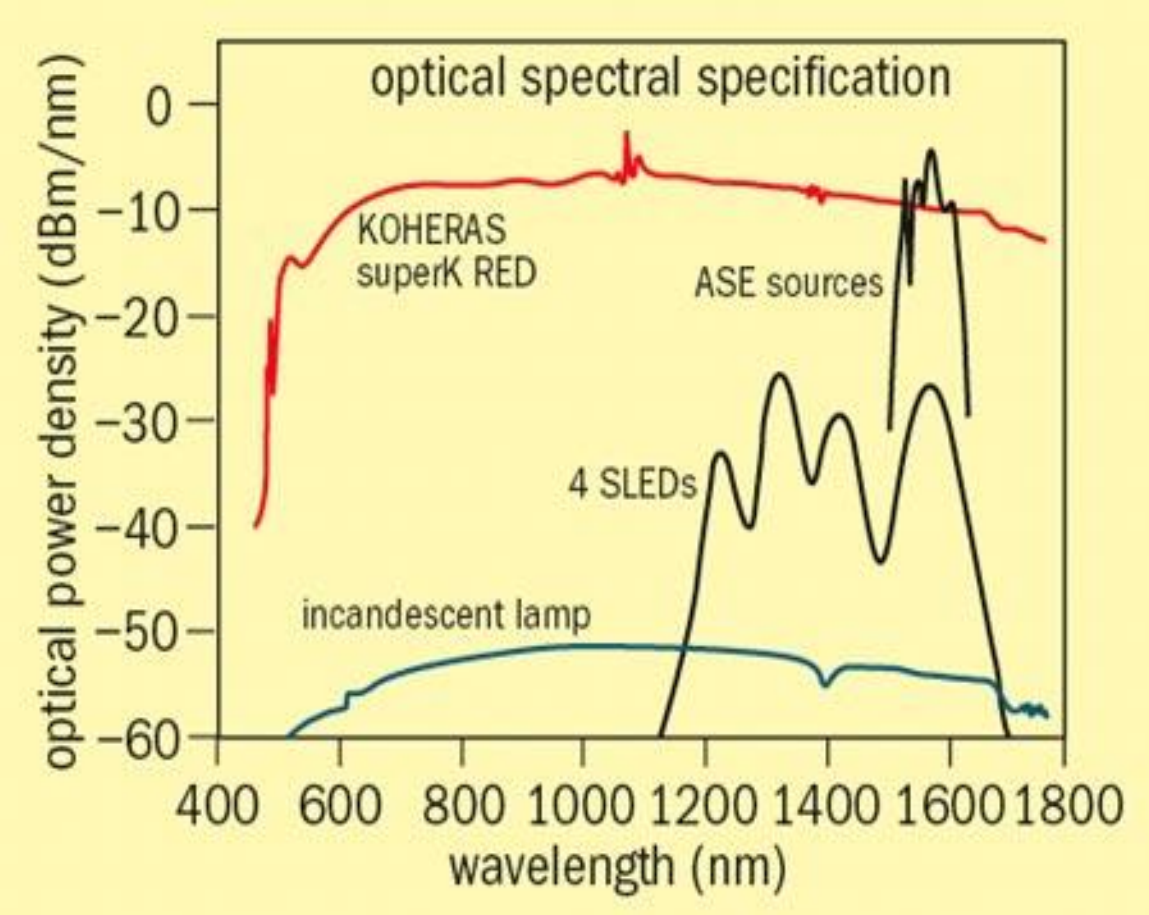

0 dBm = 1 mW
-30 dBm = 1 μW

Classical and photonic crystal fibers

1968 – fabrication of the first telecommunication fiber (*Uchida at al.)*

1996 – fabrication of the first photonic crystal fiber (*Knight at al.)*

Classical optical fiber

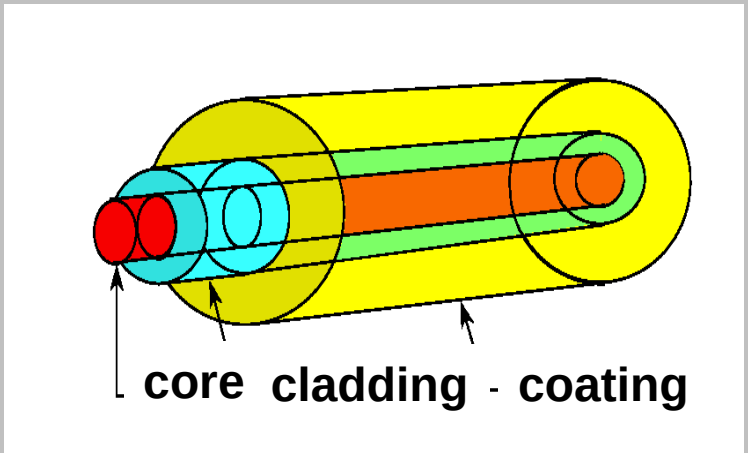

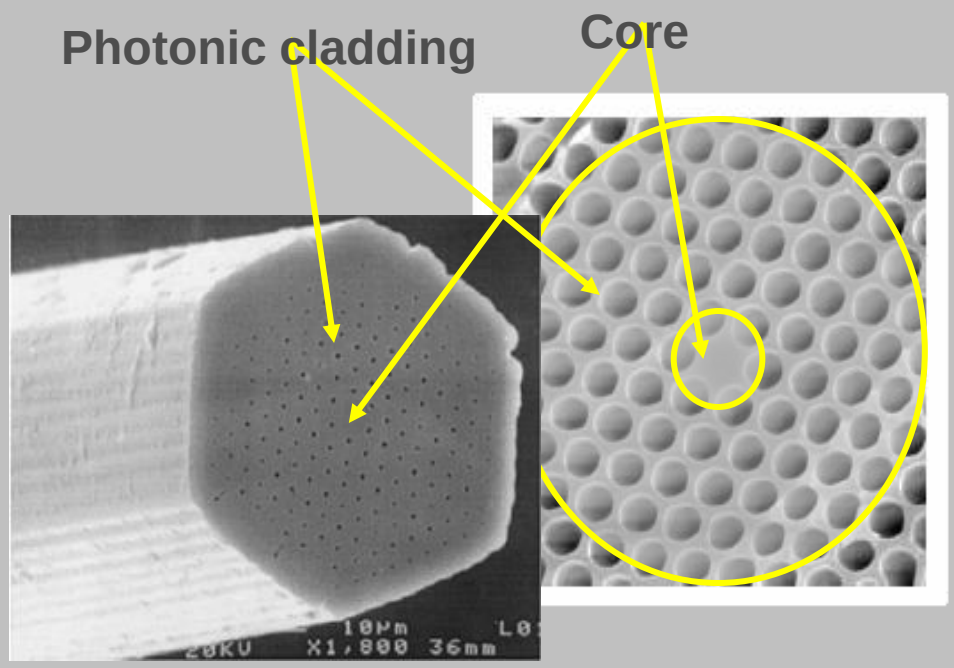

Group velocity dispersion (GVD)

Dispersion of single mode fiber

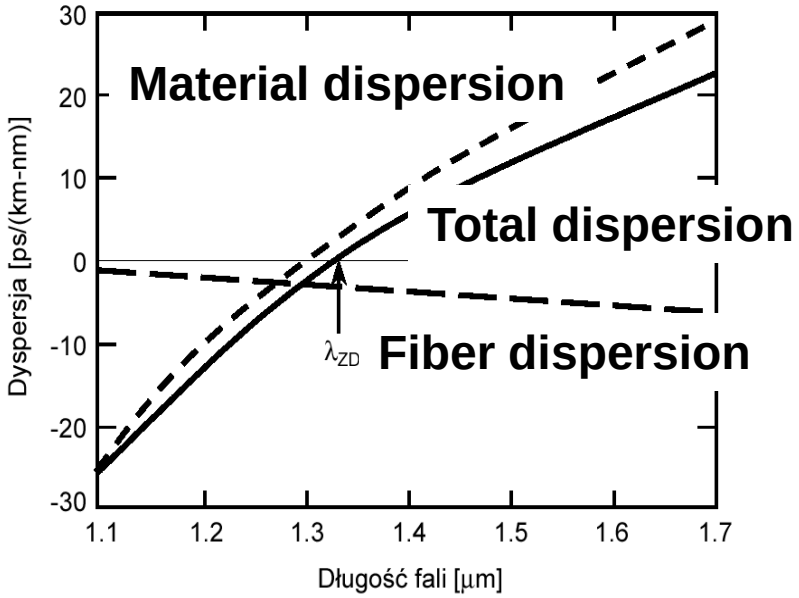

$$D = -\frac{\lambda}{c}\frac{d^2 n_{eff}}{d\lambda^2}$$

$$n_{eff} = \frac{\beta(\lambda, n_m(\lambda))}{k_o}$$

Dispersion

- **Measure of pulse spreading**
- **Commonly measured in ps.nm-1.km-1**
- **Mainly fixed by dispersion of material**
- **Can be normal (red travels faster) or anomalous (blue travels faster)**
- **Causes problems in telecommunications**

$$D(\lambda) = D_m(\lambda) + D_g(\lambda) + D_m(\lambda)$$

Modal dispersion (only multimode fibers)

Geometrical (fiber) dispersion

Material dispersion

$$D_m = -\frac{\lambda}{c}\frac{d^2 n_m(\lambda)}{d\lambda^2} \qquad D_g = -\frac{\lambda}{c}\frac{d^2 n_g(\lambda)}{d\lambda^2} = -\frac{\lambda}{c\,k_0}\frac{d^2\beta(\lambda)}{d\lambda^2}$$

Zero-dispersion shift - PCF

PCF gives unique possibilities to design dispersion in the fiber:

- **Zero-dispersion shift in the range of 650-1300 nm**
- **Positive (anomalous) dispersion for wavelengths below 1300 nm**
- **Flat dispersion in the range of a few hundred of nm.**
- **Ultra-flat dispersion**

Conventional fiber fabrication

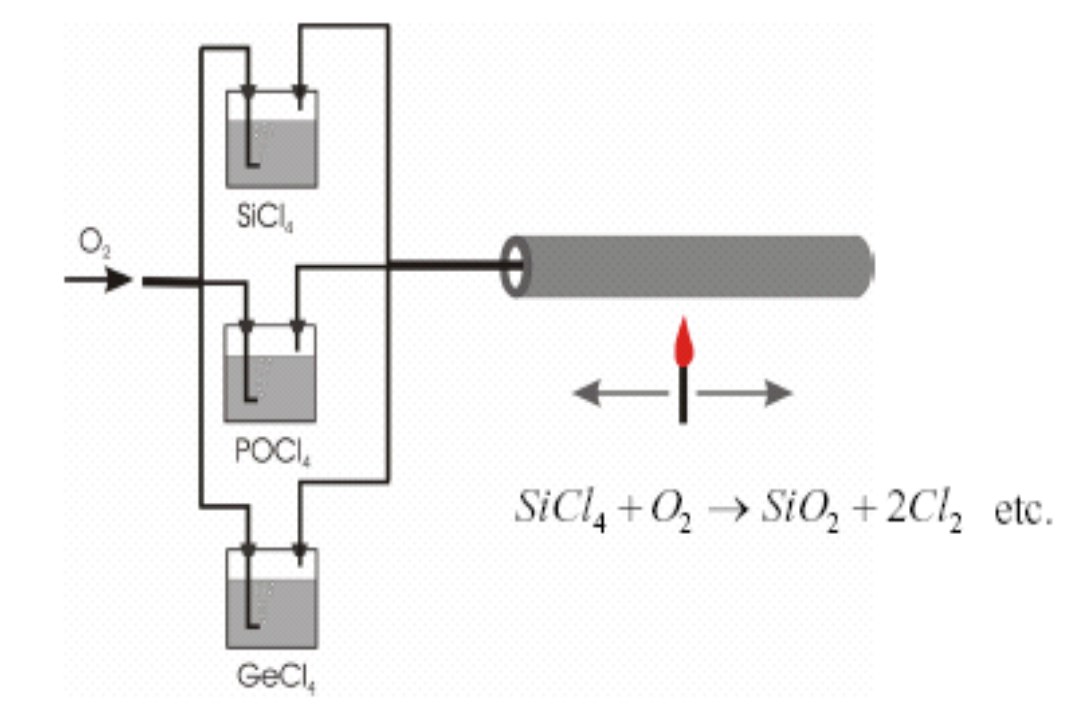

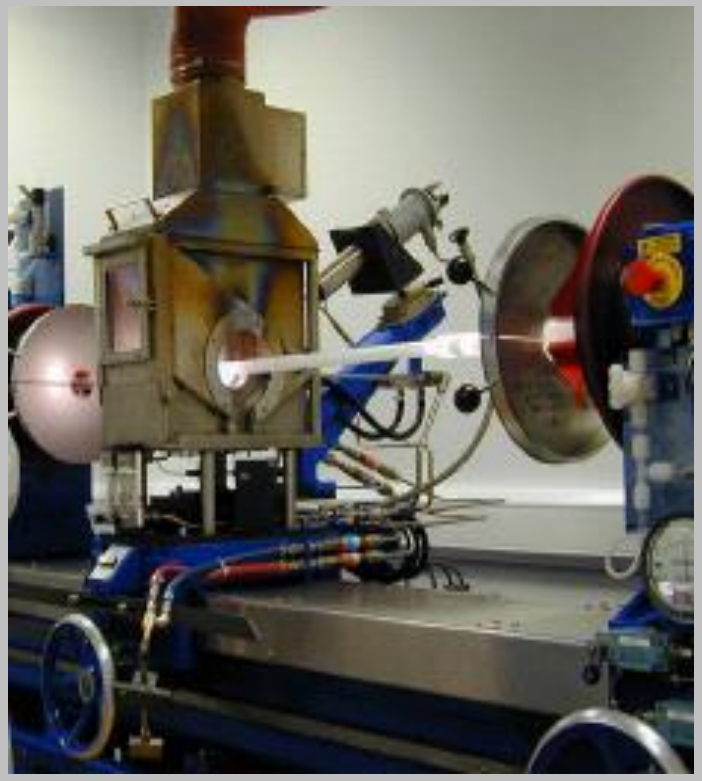

Modified chemical vapour deposition (MCVD)

J. Knight Advanced topics: Photonic crystal fiber

PCF fabrication facility – „the tower”

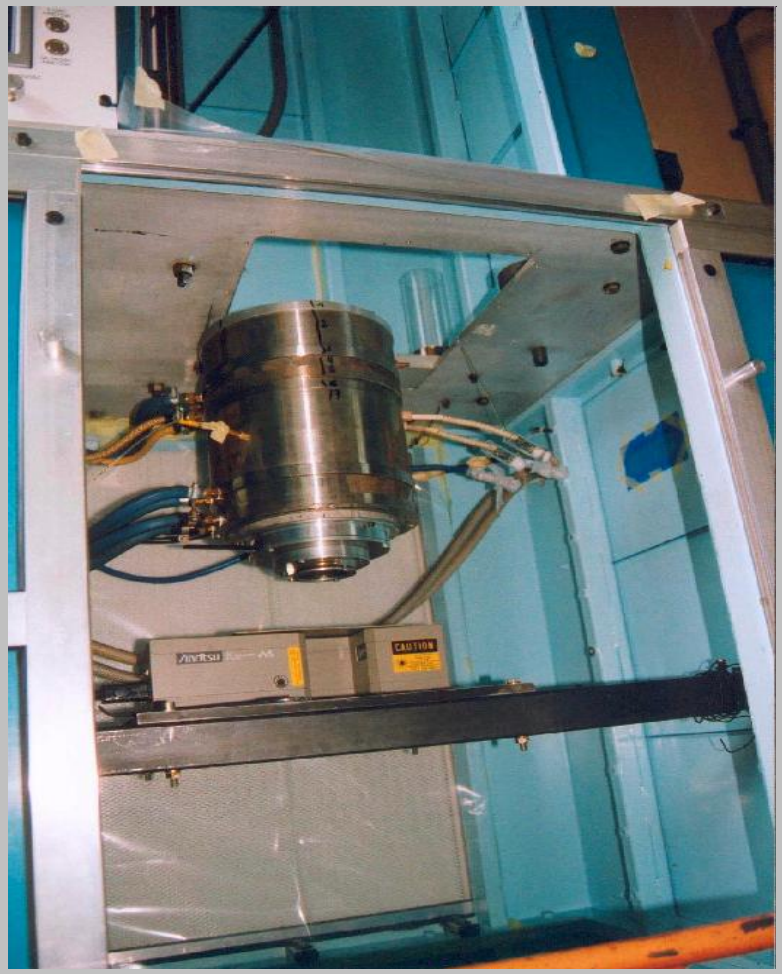

The fiber drawing tower for PCF fabrication at The Institute of Electronic Materials Technology, Warsaw, Poland

Photonic crystal fiber fabrication

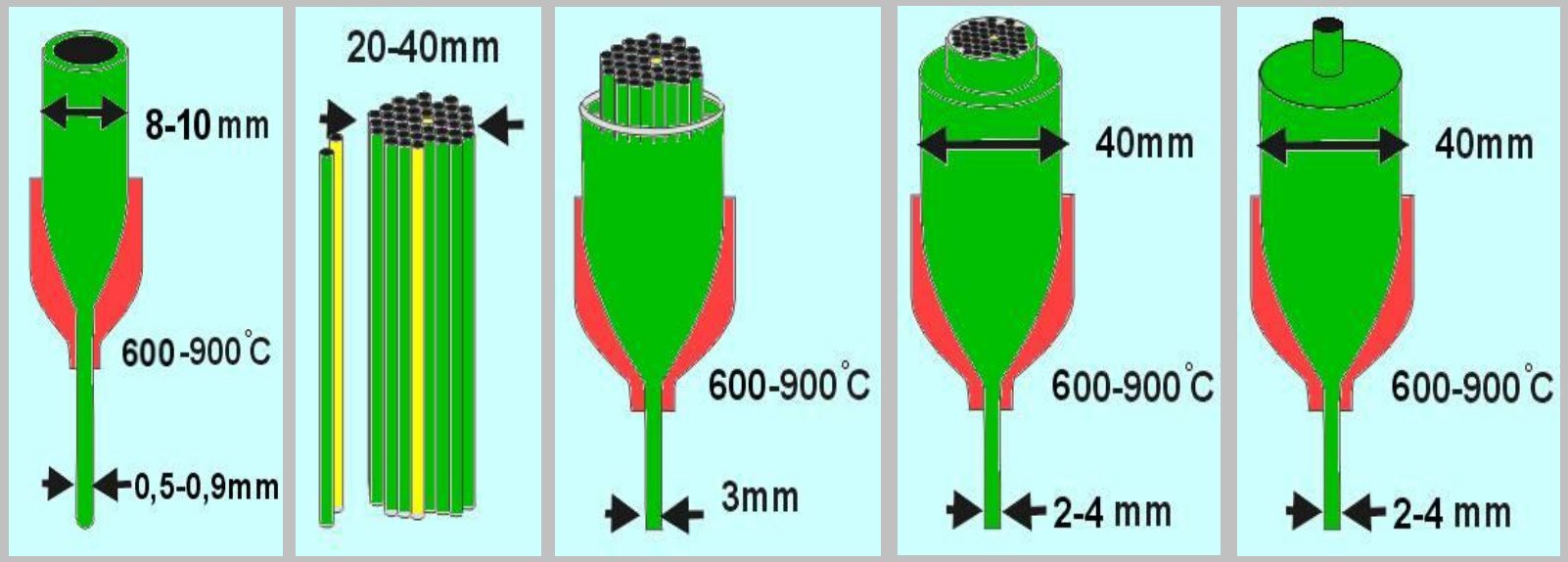

Drawing of preform elements (rods, capillaries)

Assembly of preform from basic capillaries

Subpreform drawing

Integration with tube

Fiber drawing

Technological process of photonic fiber manufacturing

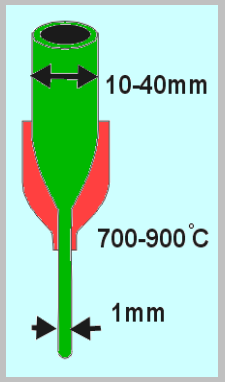

1. Drawing of elements for preform construction – glass capillaries, rods, tubes.

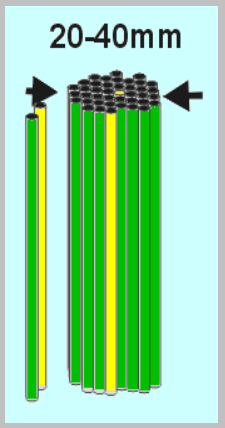

2. Macroscopic mosaic preform, with designed structure, stacking.
   At this stage we decide about type of lattice, hole/spacing ratio, distribution of capillaries, rods, etc., adding special properties elements (active, sensing, conductive, magnetostrictive, etc.) .

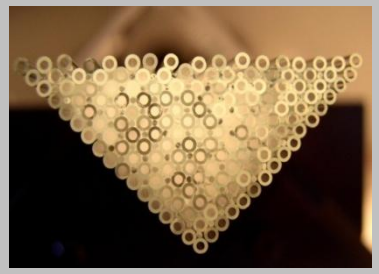

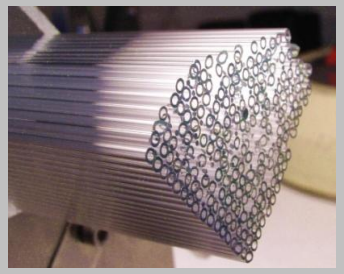

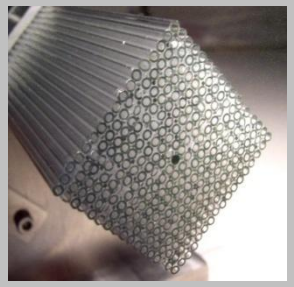

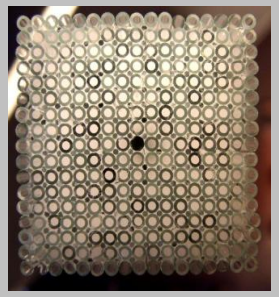

Technological process of photonic fiber manufacturing

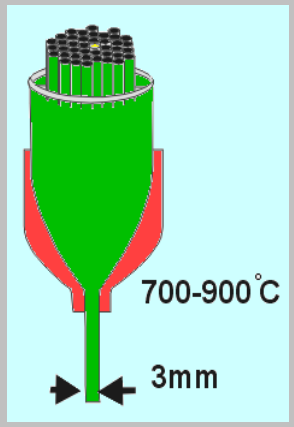

3. Intermediate (subpreform) preform drawing. Structure of subpreform is adequate to designed photonic fiber but in diameter of a few mm.

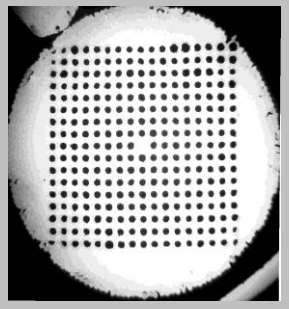

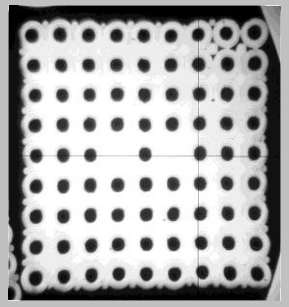

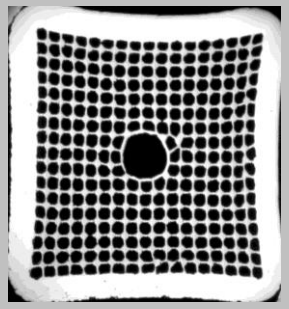

4. Arrangement of the preform for fiber drawing. Adding outside layers of glass to achieve designed dimensions of the fiber (photonic structure/fiber diameter ratio).

5. Photonic fiber drawing. At this stage we can influence to holes diameter, filling factor and fiber diameter by parameters of drawing process (temperature, feeding and drawing speeds).

SC generation in PCF NL12D1

Supercontinuum generation for pulses 100 fs, central wavelength 812 nm, fiber length 13 mm

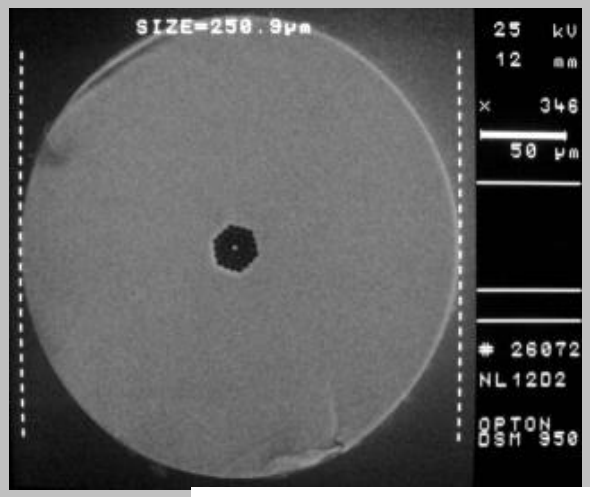

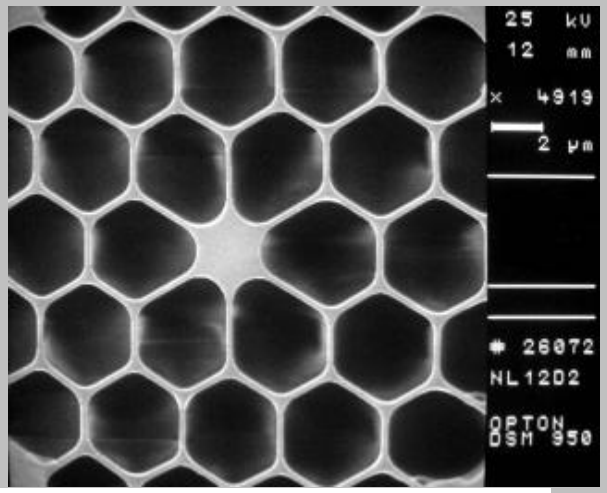

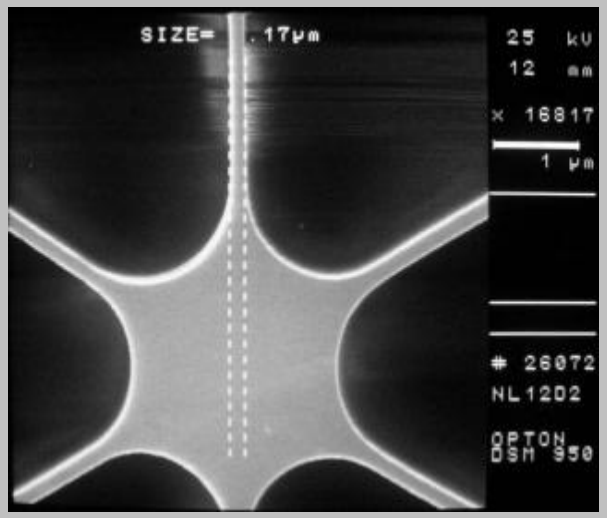

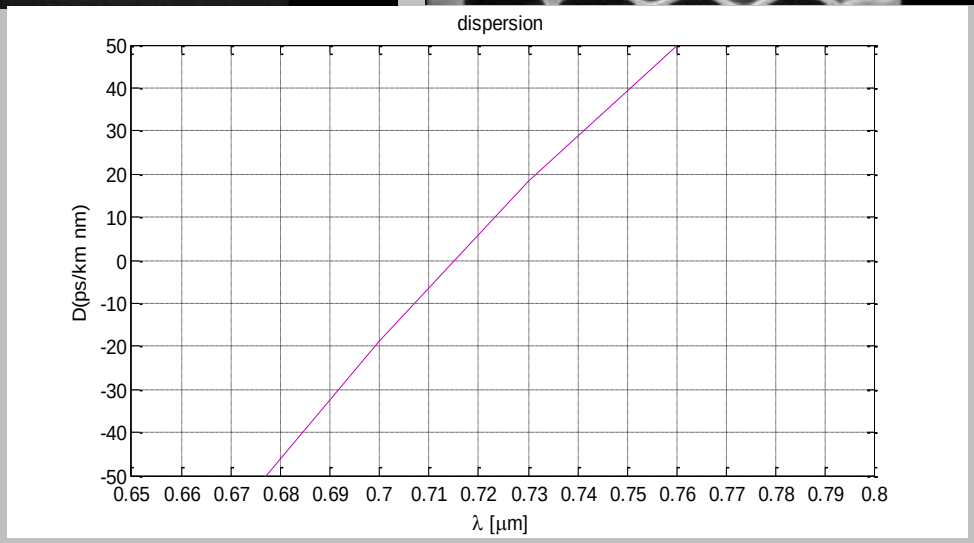

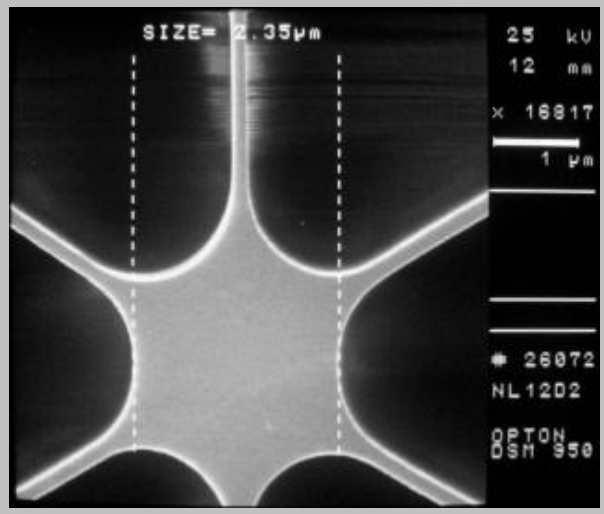

The supercontinuum spectra

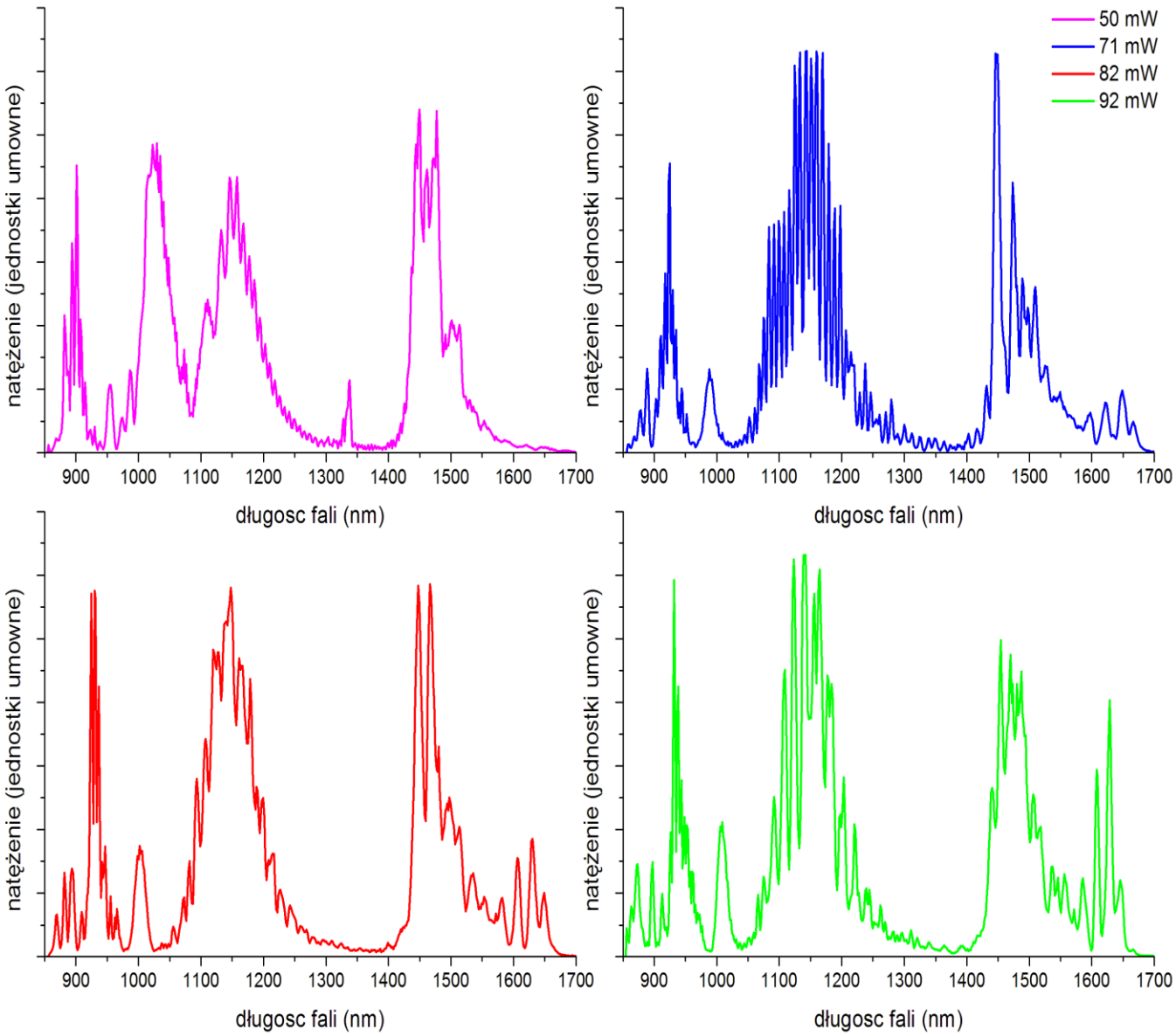

SC generation in PCF NL12A5

Supercontinuum generation for pulses 100 fs, central wavelength 755 nm, fiber length 19.5 cm

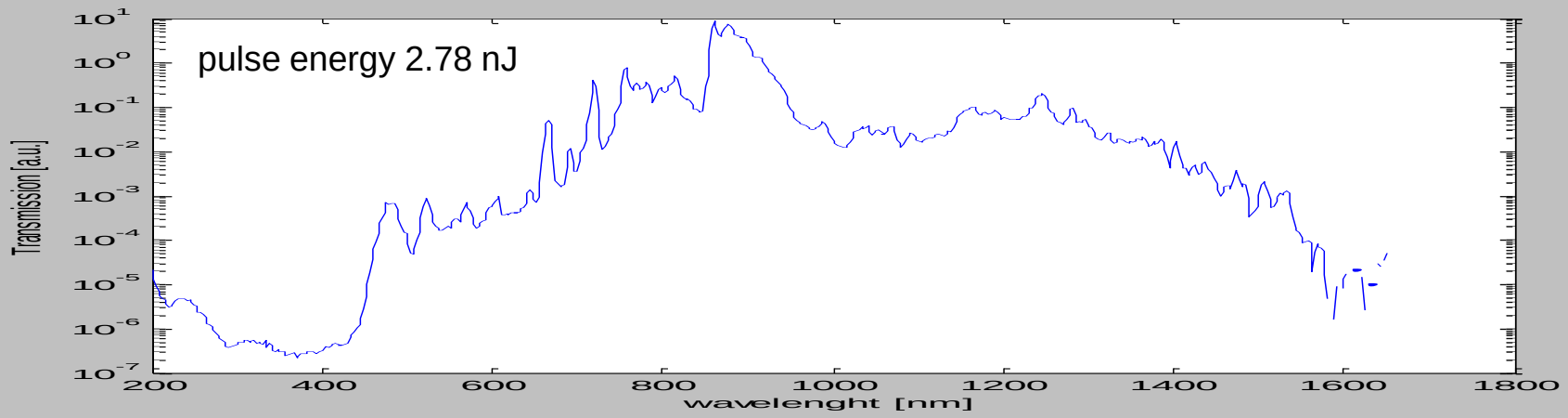

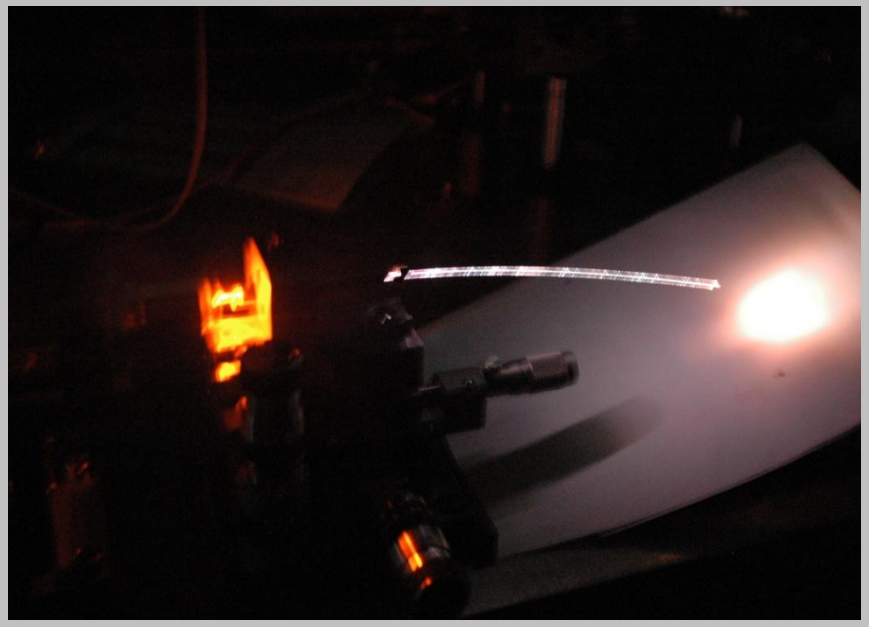

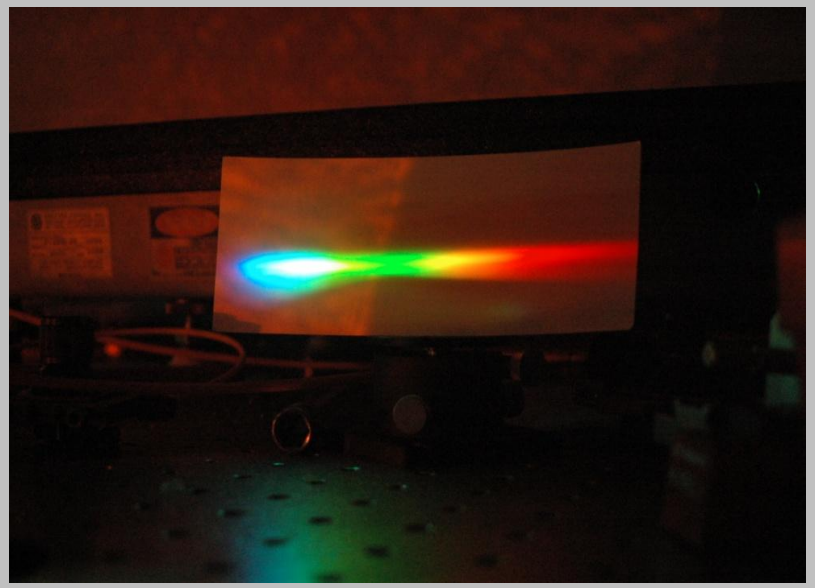

A commercial supercontinuum source (SuperK Fianium from NKT Photonics)

FEATURES

- 390-2400 nm single-mode output
- Fail-safe operation at the press of a button
- Robust and maintenance-free
- Plug & Play filter accessories